UNRAVELLING THE RESPONSES OF DIFFERENT APPLE VARIETIES TO WATER CONSTRAINTS BY CONTINUOUS FIELD THERMAL MONITORING

For: Scientia Horticulturae (Elsevier)

David Gómez-Candón[1,a], Vincent Mathieu[2], Sébastien Martinez[3], Sylvain Labbé[4], Magalie Delalande[5], Jean-Luc Regnard[5]

[1]*Institute of Agrifood Research and Technology (IRTA) Fruitcentre, Lleida, Spain*
[2]Ctifl, Centre de Balandran, Bellegarde, France
[3]Diascope, INRAe, Montpellier, France
[4] Univ Montpellier, INRAE, Montpellier, France
[5]AGAP, Univ Montpellier, CIRAD, INRAE, L'Institut Agro, Montpellier, France.
[a] email: david.gomez@irta.cat

Abstract **(308 words)**

This research aimed at analyzing the response of apple tree varieties subjected to soil water deficit and atmospheric drought in a field phenotyping platform located in the Mediterranean area. The main assumption of the study was that seasonal and daily stomatal behavior can be monitored by continuous measurement of canopy surface temperature (Ts) as a proxy of stomatal closure. To achieve the study objectives, thermal monitoring of 6 pre-commercial apple varieties was simultaneously carried out throughout one season by nadir-oriented thermo-radiometers placed 1.50m over the tree top canopy. Two water regimes were applied to each variety during a 4-week summer period: normal irrigation (WW) vs progressive water deficit (WS). The maximum difference in Ts between water regimes was recorded daily between 11:00 and 14:20 GMT, with an earlier closure of stomata in WS trees. During the day, a more negative stem water potential (Ψstem) and a higher diurnal Ts (+1° to +2°C) were observed on WS trees, resulting in a significant limitation of fruit growth. Tree water stress was caused by both edaphic and atmospheric droughts, in the medium and short terms respectively, with inter-varietal and inter-regime differences highlighting distinct stomatal closure behaviors. Results suggest that some of the varieties studied are well adapted to stressful summer conditions, as long as irrigation needs are met, while other varieties show a particular sensitivity to the mid-day evaporative demand, which may limit their extension. Although these results are not comprehensive enough to predict the optimal performance of varieties under different stress scenarios, the proposed methodology allows to assess the dynamics of tree response to water constraints using non-invasive thermal sensors. It opens up new perspectives for the phenotyping of apple cultivars under abiotic stress, achievable through the quantified study of their transpiration flux in response to stress scenarios. These prospects will require further in planta measurements to dissect varietal differences.

Keywords : Malus x domestica, non-invasive Phenotyping, Stem water potential, Stomatal regulation, Canopy surface temperature, Fruit growth

1. Introduction

Due to climate change, a general increase in temperature is expected, as well as more frequent and intense extreme weather events (IPCC, 2014). As a consequence, long periods of drought are likely to occur more frequently, especially in the Mediterranean region (Giorgi and Lionello, 2008). Climate change will have a negative impact on agricultural production in general, jeopardizing food security, both in terms of quantity and quality (Tripathi et al., 2016). In particular, climate change will threaten fruit production in temperate zones, especially where irrigation is limited (Maracchi et al., 2005), and evapotranspiration will continue to increase in response to higher climate demand. Adaptation of fruit trees to abiotic stresses such as water stress is therefore becoming an increasingly important challenge for fruit crops (Basset, 2013; Rahmati et al., 2018). In the short term, climate change is conducive to the adoption of new cropping techniques (del Pozo et al., 2019; Parajuli et al., 2019), including irrigation (Robinson et al., 2017). In the long term, the need to grow varieties that are more tolerant to climatic constraints is also expected to drive the selection of new cultivars offering greater resilience to abiotic stress and/or improved water-use efficiency (Lotfi et al., 2010; Liu et al., 2011; Lopez et al., 2017; Coupel-Ledru et al., 2019).

One of the first physiological responses of plants to water deficit is stomatal closure. This leaf response (i) induces a decrease in photosynthetic activity since the access of carbon dioxide to the mesophyll is reduced, and (ii) it limits transpiration and the dissipation of the associated latent heat of vaporization that causes (iii) an increase in the average leaf surface temperature (Tf). An indirect measure of plant response to water deficit is therefore based on an inverse relationship between Tf and stomatal opening (Fuchs, 1990). Among other authors, Maes and Steppe (2012) recalled that Tf is most often estimated by measuring the brightness temperature (Tbr) at canopy scale. Non-invasive monitoring of stomatal conductance can therefore be carried out using thermal sensors installed above canopy, which provides an early indicator of tree response to drought, since the increase in foliage temperature may occur before any other changes in plant water status (Jones, 2004). Such an approach has been successfully used for crops such as barley and black poplar to assess the stomatal sensitivity to different water regimes in a panel of varieties (Rischbeck et al., 2017; Ludovisi et al., 2017). Proximal measurement of the vegetation surface temperature requires the selection of an appropriate thermal infrared sensor (White et al., 2012). It is also important to consider the influence of the soil underlying the crop (Hackl et al., 2012; Costa et al., 2018) in order to avoid noise in the thermal signal.

Water stress at the individual tree level can be monitored by remote sensing of canopy surface temperature (Ts). For example, Gómez-Candón et al. (2016) identified higher canopy temperatures in water-stressed versus well-irrigated apple trees using thermal IR data. These authors also showed contrasting phenotypic responses to water limitation for different apple tree genotypes. Incidentally, leaf temperature varies within the entire tree canopy and spatial variability in surface temperature can be increased by water stress (Ngao et al., 2017). Selecting a representative area of interest within the canopy is therefore the first step for studying a tree's response to drought constraints over time. Issues of resolution and scale, from the leaf to individual plant and to plant cover, must be carefully resolved since the thermal signal is detected remotely, at a certain distance (Cohen et al., 2016). Thermal proxidetection can be used in a complementary manner to thermal remote sensing for cross-validation purposes, but it has also been used alone for field phenotyping of plant adaptation to drought; Thompson et al. (2018), for example, successfully used a cart equipped with a thermal camera to proximally characterize different cotton genotypes subjected to drought.

Cultivated apple (*Malus x domestica*) is mostly considered rather isohydric (Lauri et al., 2011), exhibiting fairly rapid stomatal closure in response to soil moisture deficit, which allows trees to limit transpiration and overcome short periods of drought. However, during the annual cycle, there is also an increasing tendency toward anisohydry, i.e. maintenance of stomatal opening to satisfy fruit's demand for photoassimilates, which stimulates the persistence of some photosynthetic activity until harvest (Pretorius and Wand, 2003). Lauri et al. (2016) found variable stomatal behavior in apple depending on the period of water deprivation (spring or summer), and they also showed that this species presents remarkable phenotypic plasticity under moderate stress. In addition, apple trees also have the ability to adapt to moderate drought by osmotic adjustment (Šircelj et al., 2007). Overall, however, the literature concludes that orchard irrigation deficit has a negative impact on fruit growth and resulting yield (Steduto et al., 2012).

The influence of decreasing atmospheric humidity on apple trees has been less studied. It has been shown that the resulting increase in vapor pressure deficit (VPD) promotes stomatal closure above a certain threshold value (Regnard et al., 2008; Dragoni and Lakso, 2011). Intraspecific variability in response to drought has also been recognized in *Malus x domestica*, with some commercial varieties being more or less responsive to soil moisture deficit (Massonnet et al., 2007). This also being observed in a bi-parental apple progeny(i.e., a cross between two commercial cvs : 'Starkrimson' × 'Granny Smith'), where 120 genotypes were compared (Virlet et al., 2015). It should be noted that, in these studies, genotypic variability in response to water stress has been observed in the Mediterranean area, where summer conditions that do not allow a clear differentiation between constraints

resulting from (i) the increasing soil water deficit (seasonal deficit irrigation) and (ii) the sharp drop in atmospheric humidity that occurs on a diurnal basis, repeating daily over the entire period.

The objective of this study was to evaluate the capacity of IR thermal sensors, installed on a field phenotyping platform, to monitor by continuous proximal measurement the differential behavior of a series of apple varieties subjected simultaneously to a progressive soil water deficit in summer and to the diurnal peak in atmospheric evaporative demand. It was expected that the responses of different pre-commercial apple cultivars to these abiotic stressors will help to identify the most appropriate varietal behaviors.

2. Materials and methods

In this study, carried out during summer 2015, we compared diurnal variation and seasonal evolution of thermal IR signal on 6 apple tree varieties submitted to two different irrigation regimes, a full irrigation (WW for well-watered) and a progressive water deficit (WS, for water-stressed). In parallel to the monitoring of tree canopy surface temperature (Ts), we studied two biophysical indicators during the experiment: the soil water potential (Ψsoil), which was measured twice a week, and the tree water potential (Ψstem) which was monitored periodically in its daily evolution. In addition, the effect of temporary irrigation limitation on production was addressed by seasonal monitoring of fruit growth and characterization of yield components at harvest. The irrigation supplied to each tree row, i.e., for each variety and each water regime, was monitored by water meters to ensure that the overall amounts supplied were identical. Since the study plot was located on a flat land and the trees were irrigated with micro sprinklers, runoff and drainage were considered negligible.

2.1 Study site and data acquisition

The study was carried out in the orchards of Ctifl (Interprofessional Technical Center for Fruits and Vegetables) at the Balandran station, near Bellegarde, France (N43º45’09.6”, E04º27’23.0”). The soil was a sandy clay loam, fairly homogeneous in the trial as shown by the spring resistivity maps provided by Corhize®, offering a water holding capacity of about 80mm over the 60 cm depth explored by the roots. The experimental plot, dedicated to the agronomic assessment of varieties (i.e., flowering phenology, fruit bearing habit, yield and regularity, fruit quality), was equipped in 2015 for the specific needs of the trial. The field set-up consisted of 6 rows, one row per variety, where trees were planted at a distance of 4m * 1.25 to 1.30m. The inter-rows were grassed over a width of 2 meters and regularly mowed, while the tree row was chemically weeded. In the entire experimental plot, trees were pruned, thinned and sprayed according to professional practices and the integrated fruit production guidelines. All varieties studied were grafted onto M9 rootstock and were planted as follows: Cripps Pink (2008),

Dalinette (2008), Gradiyel (2007), Inolov (2007), UEB32642 (2008) and Inored (2004). In 2015, the trees could be considered mature, in regards to vegetative development and fruit production potential, and no significant differences in canopy size were observed (data not shown).

For each apple variety, within the same row, two adjacent subplots were created: WW and WS. The trees were irrigated by a micro-sprinkler system, one emitter per tree. The individual flow rate of the micro-sprinklers was initially 46 l/h for the entire trial, with plot irrigation carefully scheduled since May 1 according to seasonal potential evapotranspiration and periodic measurement of soil water status. Starting July 2, the irrigation regime for subplots was differentiated. In the WS subplot, trees were subjected to a gradual summer soil water deficit, while irrigation of the WW subplots was maintained according to evapotranspiration (ETc) requirements twice per week. The change in irrigation regime in the WS subplot was achieved by replacing the initial 46 l/h with 24 l/h emitters (i.e. irrigation at half-rate). The trees located at the boundaries of the subplots were not considered for subsequent measurements and analyses, in order to avoid lateral water transfers between the WW and WS treatments. The differentiation between water regimes was stopped on July 30, after 4 weeks, by replacing the 24 l/h emitters in WS subplots with the original 46 l/h.

2.2 Canopy temperature measurement

The IR-120 thermo-radiometers measured canopy brightness temperature (Tbr), which was used as a proxy for canopy surface temperature (Ts). Regardless of variety, temporal variations in Ts are the result of leaf energy balance, reflecting one of Ts components, the evaporative term, which varies inversely with the tree stomatal closure in response to stressful conditions.

Ts was measured continuously on one representative tree (similar growing conditions to its neighbors) per variety and per irrigation treatment. For this purpose, IR-120 thermo-radiometers (Campbell Scientific®) were installed above the tree tops in a zenithal position. The distance between the tree tops and the thermo-radiometers was adjusted to 1.5m in order to ensure the measurement of a central canopy area with a radius of 0.50m, as shown in Figure 1. This distance was calculated using the following formula:

$$r = h * tan(\alpha) \qquad (1)$$

where h is the distance from the sensor to the top of the canopy, α is the sensor semi-angle of view (20º for the IR120) and r is the radius of the circular area spotted by the sensor. As the actual canopy radius of each of the

150 trees studied was between 0.76 to 0.94 m, which is wider than the area of interest (radius 0.50 m) measured by the
151 IR-120 sensor, the target area can be considered representative of the upper canopy.

152 The IR120 collected the average thermal signal Ts emitted by the target surface. This temperature was scanned
153 every 10 seconds, and Ts mean values were calculated and recorded every 10 minutes by a CR3000 data logger
154 (Campbell Scientific®) throughout the day. Before and after the experiment, the IR-120 thermo-radiometers were
155 carefully calibrated and verified using a blackbody device (Fluke® 9133 portable infrared calibrator). In this study,
156 canopy temperatures were only considered for full sunny days and with wind speeds below 10 $m \cdot s^{-1}$.

157 **2.3 Tree water status**

158 The stem water potential (Ψstem) is a good indicator of plant water status (Choné et al., 2001; Naor, 2006; Doltra
159 et al., 2007). Its value can vary depending on a balance between incoming and outgoing water fluxes (Simonin et
160 al., 2014). Typically, a negative minimum value of Ψstem is reached in the middle of the day when the climatic
161 demand for transpiration is maximum. Stem water potential depends on the transpiratory behavior of the variety
162 in relation to the instantaneous evaporative demand, but in WS trees, it is furthermore affected by the stress
163 experienced by the plant due to increasing soil water deficit.

164 On July 2, 16, 22 and 29, Ψstem was measured on individual leaves after 2 hours of enclosure in an aluminized
165 plastic bag designed to stop transpiration and eliminate the water potential gradient between leaf, stem, and
166 branches (Goldhamer and Fereres, 2001). Measurements were performed using a pressure chamber (model 3000,
167 Soil Moisture®) beginning at 12:00 noon solar time. Each series of measurements for the whole trial was
168 performed in the shortest time possible, approximately 45 minutes. Two trees per genotype and per treatment
169 selected for homogeneity were measured, including the individual monitored by the IR 120 sensors, at a rate of
170 three leaves per tree each time.

171 **2.4 Other data acquired**

172 In order to retrieve additional information on plant development under water irrigation treatments, environmental
173 conditions were monitored using sensors for global radiation (Rg), air temperature (Ta), air relative humidity (RH),
174 wind speed (u) and precipitation. Climatic variables were scanned every 30 s, averaged over one-hour intervals,
175 and stored using a Campbell Scientific CR10X data logger. They were used to calculate the air vapor pressure
176 deficit (VPD) among other indices. Water supply was monitored during the irrigation campaign, with water meters
177 placed at the end of each tree row, to check the homogeneity of irrigation supplies. Watermark® Soil moisture
178 probes were used to collect soil water potential (soil WP) at 0.3 m depth for Cripps Pink, Dalinette, Inored and

UEB32642 varieties (3 probes per tree). Finally, fruit growth was monitored on UEB 32642, Cripps Pink and Inored varieties. For each variety and at each date, 30 fruits were measured on two WS trees and 30 fruits on two WW trees, these trees being the same as those chosen for Ψstem measurements, and the fruits being equally distributed on the east and west sides of the row. Measurements were made once a week using a digital caliper.

2.5 Statistical analysis

One way ANOVA and Fisher's LSD *post hoc* tests were used in order to determine the effect of water regimes for all the analyzed variables. Linear regression equations and Pearson correlation coefficients were calculated to analyze the relationship between variables. Analyses were conducted using the JMP 14.2 statistical package of SAS.

3. Results

As shown in Figure 2a, the WW and WS irrigation regimes applied in July corresponded to 74% and 37% of ETo (reference evapotranspiration) respectively. The irrigation provided on the WW subplots, monitored according to the soil probes values, was mostly sufficient for tree vegetation and for satisfactory fruit growth. On WS trees, soil water deficit began on July 7 and gradually increased thereafter; cumulative WS water inputs were less than 70mm during the July restriction period. Although the trees of the studied varieties had similar vegetation characteristics at maturity (crown dimensions, same rootstock with limited root depth, and similar fruit loads), it appeared difficult to subject them to perfectly similar watering conditions, especially for the WS deficit irrigation regime.

3.1 Seasonal evolution of soil water potential and tree water status

As shown in Figure 2b, during the contrasting irrigation period, soil WP was maintained for WW trees in the range of -0.02 to -0.12 MPa for most varieties, with the exception of UEB 32642, a variety for which the WW water inputs seemed to be slightly insufficient to prevent a drop in soil WP after July 14. In WS trees, the median values recorded by the probes showed a fairly rapid decrease in soil WP, reaching the physical limit of Watermark® probes (-0.20 MPa) between July 12 to 22, depending on the variety.

The assessment of the water status of the apple trees during the experiment was mainly based on the value of Ψstem particularly that measured at solar noon, when it is typically at its lowest point. It can be observed in Figure 3 that after July 16 the varieties Inored, UEB32642 and Dalinette presented significantly more negative Ψstem values for WS trees than for WW trees, indicating an onset of water stress for the WS treatment with a progression until the end of the month resulting in final differences of -0.40 to -0.80 MPa between watering regimes. For these varieties, the midday Ψstem value at the end of July was below -1.8 MPa. For two other varieties, Cripps Pink and

Gradiyel, less differences were observed between WW and WS treatments, and in Cripps Pink, slight water stress was observed late with a midday Ψstem value below -1.6 MPa for both water regimes. No water stress was recorded in Inolov trees until July 22, while on July 29, first signs of moderate stress were detected on WS trees, with an average difference of -0.4 MPa between WW and WS irrigation regimes (Figure 3).

During the night, Ψstem and soil WP values tend to balance each other as leaf transpiration ceases and the Ψstem values retrieved at predawn (Ψpredawn, Figure S1) provides a complementary indication of the trees' water status. It was observed that Ψpredawn values corroborated the trend of developing moderate but significant water stress, consistent with the diurnal period observations, for WS trees on the three varieties Inored, UEB32642 and Dalinette, starting on July 16. For Cripps Pink variety, no significant difference was recorded between WW and WS trees (and no Ψpredawn value below -0.4 MPa), and no significant difference between WS and WW treatments were observed before July 29 for Inolov and Gradiyel varieties (Figure S1).

3.2 Apple tree canopy temperature

Seasonal evolution

It is noteworthy that the increase in Ts at midday (Table 1) occurred in accordance with the Ψstem variations previously shown (Figure 3), with the variations being inverse (the more negative the Psi stem, the higher the Ts value). Accordingly, the differences in Ts between the WS and WW treatments were appreciable from July 16 onwards. Considering all six apple varieties, there was no significant effect of water treatment WS on Ts increase. However, limiting the comparison to the three varieties that experienced moderate stress characterized by the decrease in Ψstem (Inored, UEB32642 and Dalinette), a significant difference ($P<0.01$) was obtained for the Ts between the WS and WW treatments. For each of the varieties studied, Ts at midday was always higher than the air temperature (Ta). Moreover, the average Ts at midday showed an increase comprised between +0.8° to +1.4°C for WS trees of UEB 32642 variety compared to WW trees, while this increase in Ts between the two treatments varied between +1.7° to +2.0°C for Inored, and from +1.3° to +2.0° for Dalinette (Table 1).

The variety Cripps Pink showed the lowest Ts values at solar midday, irrespective of the irrigation regime; on July 29, a difference of only +0.3 °C was found between WS and WW trees. No clear seasonal evolution of Ts-Ta or TsWS-TsWW was observed for this variety, even at the end of July, when stress conditions were starting as indicated by the slight decrease in Ψstem values previously shown for WS and WS trees (Figure 3).

Daily evolution

Regardless of the irrigation regime, nighttime Ts was lower than nighttime Ta, while the opposite was observed most of the time during the day, particularly in the afternoon. During the night, each variety presented very similar Ts values for both irrigation treatments (Figures 4.a and 4.b).

On July 4, shortly after the introduction of water restriction (WS), the diurnal evolution of Ts fitted a bell curve, regardless of the variety or the watering treatment. This evolution was in accordance with that of Ta and VPD at this date. A temporal shift was observed for thermal peaks, typically on July 20: on this date, the TsWS peak preceded the TsWW peak for UEB32642 and Inored varieties, while the time differences between Ts peaks in WS and WW trees were less consistent for Inolov and Gradiyel. On July 28, under conditions of slightly lower air temperature and lower VPD than on July 20, the same trends were observed between treatments for all varieties (Figure 4). A plateau in Ts evolution was also noticed between 12:00 and 13:00 GMT, regardless of the variety and/or the treatment.

An example representative of the daily evolution for TsWW and TsWS is shown in Figure 5 for the variety UEB32642 (July 24). A delay of 45 minutes between the maximum temperature peaks for the WS and WW treatments was noted: a TsWW maximum of 35°C was observed at 13:30, while the TsWS maximum was observed earlier, at 12:45, with higher values (36.2°C), in agreement with the values previously shown on July 20 (Figure 4a) for this variety, from the early morning. The VPD values evolved in parallel with those of Ta, with the highest VPD observed at 15:00. It should be noted that for this variety, the TsWS-TsWW difference was variable, and overall moderate; it was at its highest between 10:00 and 11:30, before the Ta and VPD peaks were reached.

The times of day at which Ts peaked for the two watering treatments and the differences in Ts max (ΔT_{max}) between the highest TsWS and TsWW are presented in Table 2 (only full sunny days have been considered). WS trees reached maximum daytime Ts value before that of WW trees in most cases, with the exception of Gradiyel variety, which did not show any sign of water stress until the end of July. The more genotypes were affected by water stress, the more pronounced the difference between TsWS and TsWW. Prior to the establishment of the irrigation restriction, the maximum Ts of WW trees was generally similar to or slightly higher than that recorded in trees intended for WS treatment (data not shown). After July 16 (i.e., 14 days after the establishment of water deficit in WS treatment) this trend reversed with increasing water stress. However, the differences between the maximum TsWS and TsWW after one month remained limited to 1.5°C (Dalinette variety).

Respective effects of water restrictions and VPD

Under the conditions of Balandran experimental platform, a strong correlation between VPD and Ta was observed at the diurnal scale, with R^2 values higher than 0.9 in the morning (from 6:00 to 13:00 GMT), and diurnal variations in VPD mainly resulting from that of Ta (data not shown). Consequently, the choice was made to plot the variations in Ts as a function of those in VPD (Figure 6a and b). The results presented for two consecutive two-day periods, chosen for comparable weather conditions, are consistent. Overall, we found that Ts differences between WS and WW trees increased linearly with more severe water constraints. Accordingly, a good correlation was also found between Ts and Ta (Figures S3.a, S3.b and S3.c), with similar differences between watering treatments (data not shown). Noticeable differences between the slopes of the regression lines (WS vs WW) were found for Inored (+0.75 to 0.81), for UEB32642 (+0.50 to 0.78) and Dalinette (+0.23 to 0.50), which were also the varieties most affected by WS irrigation regime, as shown in the previous results (soil WP and midday Ψstem and maximum daily Ts differences, Figure 3 and Table 2). For the other varieties, only slight differences were observed due to the water regime in the Cripps Pink and Inolov trees, while Gradiyel variety behaved opposite to expected, with a higher slope for the WW treatment. The slope values observed for the WW trees (Table S1) showed that the variety with the highest increase in Ts in response to the morning progression of VPD was Gradiyel, while UEB32642 was the least sensitive variety to increasing VPDs.

3.3 Fruit growth response and fruit size at harvest

During the experiment, cumulative fruit growth was monitored for the apple varieties Cripps Pink, UEB32642 and Inored (Figure 7). On July 30, at the end of the period of contrasting watering regimes, a significant limitation in fruit equatorial growth occurred on WS trees for UEB32642 and Inored varieties, compared to WW trees. For UEB32642, from 22 to 29 July, the daily growth rate under WS condition decreased to 31% (60 µm per day) of its equivalent under WW condition (190 µm per day). A similar decrease was observed in Inored, with 84 µm per day for WS against 200 µm per day for WW. No appreciable difference was found for Cripps Pink. After August 1, once water restrictions were released for the WS regime, fruit growth rates returned to similar levels in WW and WS treatments. At harvest, residual differences in fruit diameter were 2.2 mm for UEB32642 variety and 2.3 mm for Inored (Figure 7).

Table 3 shows the average fruit load and yield components at harvest. The number of fruits per tree at harvest was close to the number after thinning. The variety Cripps Pink showed a small but significant difference in individual mean fruit weight in WS trees at harvest, 9.80% (15g) higher than that of WW trees. As this difference occurred during late fruit growth, it likely resulted from initial differences in tree fruit load between treatments. For the variety UEB32642, after the fruit growth rate was reduced by water deficit in WS trees, some compensation

occurred upon return to normal irrigation conditions, since the individual WS fruit weight was reduced by only 7g (5.02%) at harvest, compared to WW, the difference in fruit yield also reflecting this residual difference. Similar results were observed for the variety Dalinette with a difference of 11g (6.32%) at harvest. For the Inored variety, the size difference noted in July for fruits on WS trees compared to WW trees was maintained to some extent until harvest, with the average fruit weight on WS trees significantly reduced by 15g (12.26%). The same trend was observed on this variety for the fruit yield in WS trees, which was reduced by 3.9 kg per tree compared to the yield of WW trees. For the Inolov variety, individual fruit weights were identical in WW and WS trees at harvest, and the difference in yield per tree (-3.4kg in WS compared to WW, not significant) probably resulted from the initial fruit load per tree. Similarly, for the variety Gradiyel, individual fruit weight at harvest was similar in WW and WS trees, while fruit yields only slightly differed, due to fruit load per tree, consistent with the lack of stress experienced by WS trees in this case.

4. Discussion

4.1. The phenotyping platform

The perspective of developing sustainable orchards with reduced input levels depends on the possibility to assess the behavior of commercial varieties under limiting conditions. In a study platform originally dedicated to assess the agronomic performance of apple tree varieties under standard conditions, we tested the relevance of introducing subplots with a temporarily reduced irrigation. Although the WS irrigation regime was similarly reduced (by -50%) for the different varieties compared to the WW regime (Figure 2a), we showed that water stress was achieved within 15 days for 3 out of 6 varieties (Inored, UEB32642 and Dalinette, Figure 3), or initiated after 1 month for one variety (Inolov), or difficult to reach for the Cripps Pink and Gradiyel varieties. These discrepancies can result from different transpiration rates specific to varieties, as stated by Beikircher et al. (2013), and/or from variable responses to drought (Virlet et al., 2015). Indeed, carrying out this study under field conditions close to those of a commercial orchard, without adjusting the irrigation regimes for each variety individually, did not allow the phenotyping to be carried out as rigorously as would have been possible with a procedure driven on phenotyping platforms with controlled-conditions. It should be noted, however, that it is not possible to compare mature fruiting trees on such platforms due to the adult tree size. The challenges posed by field phenotyping technologies have been addressed in many previous research studies such as White et al. (2012), Araus and Cairns (2014) and Deery et al. (2014).

Equipping the field phenotyping platform with a device for continuous collection of canopy temperature data has enabled high-precision thermal monitoring of plants facing hydric constraints. Simultaneous acquisitions on a series of varieties relied on the use of non-invasive sensors capable of performing automatic measurements, as highlighted by Costa et al. (2019). We demonstrated here the interest of using thermoradiometers carefully calibrated before and after the experiment, and connected to data acquisition systems (two CR3000 data loggers). Monitoring of a larger number of varieties than in this study would require the use of a multiplexed acquisition system.

4.2. Soil and atmospheric effects

Canopy surface temperature Ts that was monitored on apple trees was related to the water stress they experienced, and regulated by stomatal closure in response to this constraint (Jones et al., 2002). Stomatal regulation was affected in this experiment by both edaphic and atmospheric components, i.e. soil water deficit and air vapor pressure deficit. Taking these two factors into account, two-time scales were distinguished: the tree seasonal response to the increasing soil water deficits throughout July, and the daily and morning response of the tree to increase in air temperature (Ta) and decrease in relative humidity (RH) reflected by an increase in VPD. Thus, the two main causes of Ts variations were the irrigation shortage (medium term effect) and the high evaporative atmospheric demand during sunny days (short term effect).

As concerns seasonal evolution, both availability of soil water and atmospheric demand have influenced the plant foliar functions. Considering that the atmospheric evaporative demand at each moment affected equally all the plants studied in the same way, whatever the irrigation treatment, the most important differentiating factor in the trial was the amount of water available in the soil. Differences in Ts responses to WS vs WW water regimes were typically traduced by steeper slopes in the Ts/VPD graphs (Figure 6) for the three varieties where water stress was reached, i.e., Inored, UEB32642 and Dalinette (Fig 6b vs 6a).

On a daily scale, the amount of soil water available can be considered only slightly variable, so that variation in atmospheric evaporative demand is the most important factor determining stomatal regulation in the short term. In our study, it was observed that WW and WS trees presented similar Ts patterns at the beginning of the day (Figure 4a and 4b) and at the end of the afternoon, showing that differences in behavior between varieties are the result of the effect of the central hours or the day, as stated in previous studies such as Costa et al. (2018). A rapid rise in Ts first occurred in the morning, resulting from rapid stomatal closure, so that in the middle of the day a maximum

Ts was observed. Interestingly, the canopy temperature peaks were reached at different times, depending on the water regime. The Ts peak was followed by a plateau period, typically after 1:00pm. As the difference between the daytime Ts and Ta gradually decreased during the second half of afternoon (Figure 4), regardless of the irrigation regime, it can be assumed that some stomatal conductance was maintained until dusk, before an almost complete stomatal closure at night time. The fluctuations in Ts in response to diurnal variations in VPD and Ta constitute a proxy for stomatal response, and illustrate the phenotypic plasticity of the apple species (Lauri et al., 2016). Since Ts elevation (or stomatal closure) in response to increasing VPDs was particularly noticeable in the morning, we considered that the differences in varietal sensitivity to VPD could be analyzed and inferred from the differences in Ts/VPD slopes shown in Figure 6. In this respect, based on what was observed on the WW trees, the most sensitive variety to the increase in VPD were Gradiyel and Inolov, while UEB32642 showed the lowest increase in Ts in response to increasing VPD (Figures 6a and b, Table S1). The morning increase in TsWW, correlated with that of VPD (Figure 6a and b), occurred at a rate revealing a greater decrease in transpiration in response to greater air dryness, depending on the variety, while differences in slope of the regression lines between the WS and WW treatments traduced the additional effect specifically attributable to soil desiccation. The greater the difference in slope, the greater the reduction in transpiration rate resulting from the soil water deficit. To our knowledge, no scientific study has yet been published on continuous thermal monitoring of the canopy to assess the diurnal stomatal behavior of water-stressed apple varieties.

The characteristic Ts peak that was observed earlier in WS trees than in WW trees at midday time can be interpreted in terms of earlier stomatal regulation in the former (Table 2 and Figure 5). This probably results from stressful conditions that add up earlier in the WS treatment: higher leaf temperature, lower leaf water potential, all of which contribute to reduced stomatal conductance (Jarvis, 1976). During the afternoon, differences between hydric conditions become progressively less marked with a parallel decrease in Ta and VPD. Accordingly, smaller differences in Ts were observed at this moment between the two irrigation regimes. Overall, the midday Ts values observed in WS treatments evolved during the experiment in accordance with those of Ψstem (Figure 3, Figure S2) where an increment of Ts is associated to a decrease in Ψstem (Wang and Gartung, 2010, González-Dugo et al., 2012).

As proxy-detection performed for canopy temperature sensing was relative to the top of the tree, further research could be carried out more in depth, considering the whole apple canopy microclimate for different varieties. Ngao et al. (2017) through a modeling approach on apple leaf temperature showed that the temperature differences at

379 the top of canopy between stressed and unstressed trees are smaller than the equivalent differences averaged over
380 the whole crown. Moreover, other authors like González-Dugo et al. (2012) found that intra-crown temperature
381 variability in almond trees can be a useful marker of the onset of water stress, being increased for medium water
382 stress conditions. Variations in Ts depend on (i) the amount in water available in the soil and (ii) microclimatic
383 variations in evaporative demand (Kullaj and Thomaj, 2019). The atmospheric evaporative demand within the
384 WW tree crowns could be lower since the humidity of inner canopy is itself dependent on the transpiration rate,
385 which can be locally higher, and soil evaporation in WW can also contribute to the local increase in air humidity.
386 Thus, WS trees where soil evaporation is lowered are probably subject to more stressful conditions. However,
387 although different soil water loss effects were observed between varieties and treatments, atmospheric demand
388 (high VPD values) often appeared as the prevailing effect. The specific VPD effect is appreciable in Figures 6 a
389 and b and Table S1, where a strong linear relationship between Ts and VPD was shown, the differences between
390 watering treatments being more evident in the first hours of the day. Soil drought resulted in a greater rate of
391 increase in Ts in WS trees, compared to WW, which was likely the result of an earlier stomatal closure.

392 **4.3. Varietal responses to water stress**

393 Although continuous monitoring of transpiration flux per tree, leaf stomatal conductance and net photosynthesis
394 were not carried out directly in this field trial, and a similar level of water stress was not achieved for all varieties,
395 it is tempting to use the variables acquired to draw a first set of conclusions. Regarding the response of apple
396 varieties to seasonal conditions of progressive water deficit, we can differentiate some behaviors. The analysis of
397 varietal responses to soil water deficit and high VPD conditions was made possible by examining Figure 6 a and
398 b: a particular sensitivity to soil desiccation was shown in UEB32642 and Inored and to a lesser extent in Dalinette,
399 while Gradiyel and Inolov revealed a notable sensitivity to diurnal increase in VPD. UEB32642 and Cripps Pink,
400 on the other hand, showed a limited response to increasing VPD. Moreover, as the maximum Ts was observed
401 earlier for trees submitted to WS regime compared to WW ones in most cases (Figures 4 and 5, Table 2), it can be
402 deduced that soil water deficit and VPD have exerted additional effects (starting in mid-July) most likely causing
403 earlier stomatal regulation in WS trees, consistent with observations in previous studies (Kullaj and Thomaj, 2019).
404 This was particularly noticeable in the Inored variety, and to a lesser extent in UEB32642.

405 Plants have developed various soil drought adaptation processes in order to limit a dramatic decrease in leaf water
406 potential under stressful conditions. As a result, contrasting controls of leaf water potential have been observed
407 across species when submitted to similar soil water deficit conditions (Tardieu and Simonneau, 1998). The so-

called isohydric species efficiently maintain high leaf water potential when the soil dries, whereas anisohydric species cannot prevent leaf water potential from dropping. Contrasts also exist between varieties within the same species, as shown in grapevine (Schultz, 2003) and apple tree (Massonnet et al., 2007). It has been proposed that the variation between plant stomatal behaviors, and subsequent carbon gain vs water loss, can mainly result from how stomatal pores at the leaf surface close under water deficit and control plant transpiration (Buckley, 2005). A series of recent studies have also highlighted the underlying complexity of stomatal movements, which responds to various environmental and physiological components at different spatial and temporal scales. As a result, under given conditions, there could be a continuum between rather isohydric or rather anisohydric species and varieties (Klein, 2014). Furthermore, Franks et al. (2007) reported that isohydric or anisohydric behavior could vary throughout the season, depending on plant hydraulic features of the whole plant, producing the so-called isohydrodynamic response, while the sink activity of developing fruits increases the demand for carbon assimilates and stimulates stomatal opening and thus temporary anisohydry until the harvest.

In general, it is recognized that a rather anisohydric behavior is favorable to carbon assimilation, allowing for better plant performance and yield in the case of short-term water deficits (or irrigation failure), whereas rather isohydric behavior is favorable in the case of longer term water rationing, since it leads to water saving and plant resilience if carbon starvation is not excessive (McDowell, 2011). In the perspective of this work, it could be interesting to conclude more definitely on the varietal behaviors by performing more thorough ecophysiological characterization of the trees, at different periods of their cycle, and to introduce the particular sensitivity to air drought as an additional environmental stress factor (Šircelj et al., 2007), limiting the cultivation possibilities for the most sensitive varieties (Gradiyel in particular).

Regarding tree production, the moderate effect of water deficit on yield and fruit size at harvest (Table 3) can be explained by the short duration of water deficit period compared to the complete cycle from flower to fruit. The limiting effect of water deficit on fruit growth was observed in the short term on Inored and UEB32642 (Figure 7), but it was partly compensated in the long term, a phenomenon also observed by Lopez et al. (2018). The osmoprotective capacity of the apple trees (Li et al. 2012) may have enabled these varieties to overcome moderate temporary stress conditions and to recover after the limiting conditions were removed.

4.4. Practical consequence for tree phenotyping and future investigation

435 The acquisition of thermal data using non-invasive proxidetection sensors shows promise for the assessment of
436 plant water stress, even where differences between growing conditions are small (Sánchez-Virosta et al., 2020). It
437 has been shown that canopy temperature is a reliable proxy for stomatal conductance in vineyards (Leinonen et
438 al., 2006) and that continuous thermal monitoring is useful to assess the dynamics of canopy response to non-
439 optimal growing conditions. Thus, plant canopy temperature responds specifically to changes in stem water
440 potential. This effect has already been studied since the 1970s (Ehrler et al., 1978). This relationship is not direct
441 and depends on more factors, such as air temperature. This study also demonstrates the importance of choosing
442 the best time for the acquisition of Ts (as proxy of canopy stomatal conductance) in order to effectively detect the
443 intensity of its variations in response to water constraints. In this study, the maximum Ts difference between
444 irrigation treatments was recorded between 11:00 to 14:20 GMT. After solar midday, Ts tended to reach similar
445 values for WW and WS trees, which is an agreement with the measured Ψstem values.

446 This experiment was limited to the comparison of six cultivars, but it could be extended to a wider range of
447 varieties, considering pre-commercial varietal assays. In this perspective, a very interesting approach to develop
448 over this type of multi-varietal trial could be carried out by a drone equipped with a thermal sensor that would
449 allow remote thermal acquisitions over an entire experimental field. But this will rely on a careful choice of flight
450 times for the aerial vehicle, as well as the determination of flight frequency and revisit time.

451 In this study, the trees' Ts were acquired at the top of the canopy. But it should be noted that the microclimatic
452 conditions within the tree canopy, more humid, can influence the local evaporative demand. As a consequence,
453 obtaining a more complete picture of canopy thermal responses could involve, in parallel to the aerial detection,
454 the joint use of multiple air temperature and relative humidity sensors, and/or the use of structural-functional plant
455 models satisfactorily parameterized (Ngao et al., 2017).

456 Future research could include more extensive measures in planta, including sap flow (Do et al., 2011), even not
457 easy to perform in multi-varietal assays, and/or the dynamic measurement of tree water potential with innovative
458 sensors, such as the leaf mini-probes used by Martinez-Gimeno et al. (2017). Continuous monitoring of the xylem
459 potential of individual trees could finally be based on the use of micro-tensiometers recently released and tested
460 in vineyards (Pagay, 2021).

5. Conclusions

High-throughput field phenotyping techniques help breeders to choose the varieties best adapted to local climatic conditions. In water stressed plants, stomatal closure is induced, which reduces plant transpiration and carbon uptake and may lead to yield losses. In this study, temporary soil water deficit was applied to a series of apple varieties, and their behavior was compared, making use of continuous canopy thermal assessment as a proxy for stomatal closure. Comparison between water regimes in the field suggested differences in time-course stomatal closure related to air diurnal evaporative demand and to seasonal edaphic conditions. The most affected genotypes by medium-term irrigation restriction were Inored, UEB32642 and Dalinette and Inored, while Cripps Pink and Gradiyel were much less affected, and Inolov showed an intermediate behavior. The variety Gradiyel showed a particular sensitivity to high evaporative demand, which does not allow it to be recommended for cultivation in the Mediterranean area.

In future studies on plant water stress response, it will be important to choose the right day time for acquisition of biophysical proxies (either Ψstem, Ts, etc.) relative to stress. In this work, we concluded that most marked differences among irrigation treatments were recorded each day between 11:00 and 14:20 GMT, with an earlier closure of stomata in trees submitted to water restriction.

The methodology proposed makes it possible a dynamic estimation of tree response to water constraints using non-invasive thermal sensors. Moreover, as genotypic differences were found between the water regimes studied, it seems promising for high-throughput field phenotyping. In future studies, it will be interesting to carry out more extensive in planta measurements to finely dissect varietal differences and infer their adaptive capacities to different climate scenarios.

Author contributions

David Gómez-Candón and Jean-Luc Regnard both designed the study methodology, being helped by the proposals of Sylvain Labbé. D.G.-C. and J.-L.R. carried out part of the field work, which was hosted and facilitated by Vincent Mathieu and his colleagues, at the Balandran Ctifl Center. Sébastien Martinez and Magalie Delalande were heavily involved in the equipment of the experimental plot and participated in the experimental work. D.G.-C. performed the data extraction and analysis and wrote the original draft of the paper, which was revised and edited by J.-L.R.

Acknowledgements

Financial support from the French Ministry of Agriculture. Casdar C-2014-10 (Aliage-fruits project, 2014-17) is gratefully acknowledged. Laurent Albrech, Audrey Jolivot, Fanny Deboisvilliers and Arnaud Pintault are acknowledged for scientific and technical support.

References

Araus, J.L., Cairns, J.E., 2014. Field high-throughput phenotyping: the new crop breeding frontier. Trends Plant Sci. 19, 52-61. https://doi.org/10.1016/j.tplants.2013.09.008

Basset, C.L., 2013. Water use and drought response in cultivated and wild apples. In: Vahdati K., Leslie C. (Eds), Abiotic stress - plant responses and applications in agriculture. InTech, Rijeka (Croatia), pp. 249-275. http://dx.doi.org/10.5772/55537

Beikircher, B., De Cesare, C., Mayr, S., 2013. Hydraulics of high-yield orchard trees: a case study of three *Malus domestica* cultivars. Tree Physiol. 33, 1296-1307. https://doi.org/10.1093/treephys/tpt096

Buck, A.L., 1981. New equations for computing vapor pressure and enhancement factor. J. Appl. Meteorol. 20, 1527-1532. https://doi.org/10.1175/1520-0450

Buckley, T.N., 2005. The control of stomata by water balance. New Phytol. 168, 275-292. https://doi.org/10.1111/j.1469-8137.2005.01543.x

Choné, X., Van Leeuwen, C., Dubourdieu, D., Gaudillère, J.P., 2001. Stem water potential is a sensitive indicator of grapevine water status. Ann. Bot. 87, 477-483. https://doi.org/10.1006/anbo.2000.1361

Cohen, Y., Alchanatis, V., Saranga, Y., Rosenberg, O., Sela, E., & Bosak, A., 2016. Mapping water status based on aerial thermal imagery: comparison of methodologies for upscaling from a single leaf to commercial fields. Precision Agric. 18, 801–822. https://doi.org/10.1007/s11119-016-9484-3

Costa, C., Schurr, U., Loreto, F., Menesatti, P., Carpentier, S., 2019. Plant phenotyping research trends, a science mapping approach. Front. Plant Sci. 9, 1933. https://doi.org/10.3389/fpls.2018.01933

Costa, J. M., Egipto, R., Sánchez-Virosta, A., Lopes, C. M., Chaves, M. M., 2018. Canopy and soil thermal patterns to support water and heat stress management in vineyards. Agric. Water Manag. 216, 484-496. doi:10.1016/j.agwat.2018.06.00

Coupel-Ledru, A., Pallas, B., Delalande, M., Boudon, F., Carrié, E., Martinez, S., Regnard, J.L., Costes, E., 2019. Multi-scale high-throughput phenotyping of apple architectural and functional traits in orchard reveals genotypic variability under contrasted watering regimes. Hortic. Res. 6, 52. doi:/10.1038/s41438-019-0137-3

Deery, D., Jimenez-Berni, J., Jones, H. G., Sirault, X., Furbank, R., 2014. Proximal remote sensing buggies and potential applications for field-based phenotyping. Agronomy, 5, 349-379. https://doi.org/10.3390/agronomy4030349

del Pozo, A., Brunel-Saldias, N., Engler, A., Ortega-Farias, S., Acevedo-Opazo, C., Lobos, G.A., Jara-Rojas, R., Molina-Montenegro, M.A., 2019. Climate change impacts and adaptation strategies of agriculture in mediterranean-climate regions (MCRs). Sustainability, 11, 2769. https://doi.org/10.3390/su11102769

Do, F.C., Ayutthaya, S.I.N., Rocheteau, A., 2011. Transient thermal dissipation method for xylem sap flow measurement: implementation with a single probe. Tree Physiol., 31, 369-380. https://doi.org/10.1093/treephys/tpr020

Doltra J, Oncins JA, Bonany J, Cohen M (2007) Evaluation of plant-based water status indicators in mature apple trees under field conditions. Irrig. Sci. 25, 351–359. https://doi.org/10.1007/s00271-006-0051-y

Dragoni, D., Lakso, A.N., 2011. An apple-specific ET model. Acta Hortic. 903, 1175–1180. https://doi.org/10.17660/actahortic.2011.903.164

Ehrler, W.L., Idso, S.B., Jackson, R.D., Reginato, R.J., 1978. Wheat canopy temperature: relation to plant water potential. Agron. J., 70, 2, 251-256. https://doi.org/10.2134/agronj1978.00021962007000020010x

Franks, P.J., Drake, P.L., Froend, R.H., 2007. Anisohydric but isohydrodynamic: seasonally constant plant water potential gradient explained by a stomatal control mechanism incorporating variable plant hydraulic conductance. Plant Cell Environ. 30, 19-30. https://doi.org/10.1111/j.1365-3040.2006.01600.x

Fuchs, M., 1990. Infrared measurement of canopy temperature and detection of plant water-stress. Theor. Appl. Clim. 42, 253-261. https://doi.org/10.1007/BF00865986

Giorgi F., Lionello P., 2008. Climate change projections for the mediterranean region. Glob. Planet. Change, 63, 90-104. https://doi.org/10.1016/j.gloplacha.2007.09.005

Goldhamer D.A., Fereres E., 2001. Irrigation scheduling protocols using continuously recorded trunk diameter measurements. Irrig. Sci. 20, 115–125. https://doi.org/10.1007/s002710000034

Gómez-Candón, D., Virlet, N., Labbé, S., Jolivot, A., Regnard, J.L., 2016. Field phenotyping of water stress at tree scale by multispectral UAV-sensed imagery: New insights for thermal acquisition and calibration. Precis. Agric. 17, 786–800. https://doi.org/10.1007/s11119-016-9449-6

González-Dugo, V., Zarco-Tejada, P., Berni, J. A. J., Suárez, L., Goldhamer, D., Fereres, E., 2012. Almond tree canopy temperature reveals intra-crown variability that is water stress-dependent. Agr. Forest Meteorol. 154-155, 156-165. https://doi.org/10.1016/j.agrformet.2011.11.004

Hackl, H., Baresel, J.P., Mistele, B., Hu, Y., Schmidhalter, U., 2012. A comparison of plant temperatures as measured by thermal imaging and infrared thermometry. J. Agron. Crop Sci. 198, 415–429. https://doi.org/10.1111/j.1439-037X.2012.00512.x

IPCC (Intergovernmental Panel on Climate Change), 2014. Climate Change 2014: Impacts, adaptation, and vulnerability. Cambridge, UK: Cambridge University Press, 2014. https://doi.org/10.1017/CBO9781107415386

Jarvis, P.G., 1976. The interpretation of the variations in leaf water potential and stomatal conductance found in canopies in the field. Phil. Trans. Royal Soc. London, B 273, 593-610. https://doi.org/10.1098/rstb.1976.0035

Jones, H. G., Stoll, M., Santos, T., de Sousa, C., Chaves, M. M., Grant, O. M., 2002. Use of infrared thermography for monitoring stomatal closure in the field: application to grapevine. J. Exp. Bot. 53, 2249–2260, https://doi.org/10.1093/jxb/erf083

Jones, H.G., 2004. Irrigation scheduling: Advantages and pitfalls of plant-based methods. J. Exp. Bot. 55, 2427-2436. https://doi.org/10.1093/jxb/erh213

Klein T., 2014. The variability of stomatal sensitivity to leaf water potential across tree species indicates a continuum between isohydric and anisohydric behaviours. Funct. Ecol. 28, 1313-1320. https://doi.org/10.1111/1365-2435.12289

Kullaj, E., Thomaj, F., 2019. A novel screening method in breeding apples for optimal stomatal behaviour. Acta Hort., 1261, 39–46. doi:10.17660/ActaHortic.2019.1261.8

Lauri, P.É., Gorza, O., Cochard, H., Martinez, S., Celton, J.M., Ripetti, V., Lartaud, M., Bry, X., Trottier, C., Costes, E., 2011. Genetic determinism of anatomical and hydraulic traits within an apple progeny. Plant Cell Environ. 34, 1276-1290. https://doi.org/10.1111/j.1365-3040.2011.02328.x

Lauri, P.É., Barigah, T.S., Lopez, G., Martinez, S., Losciale, P., Zibordi, M., Regnard, J.L., 2016. Genetic variability and phenotypic plasticity of apple morphological responses to soil water restriction in relation with leaf functions and stem xylem conductivity. Trees 30, 1893–1908. https://doi.org/10.1007/s00468-016-1408-3

Leinonen, I., Grant, O.M., Tagliavia, C.P.P., Chaves, M.M., Jones, H.G. 2006. Estimating stomatal conductance with thermal imagery. Plant, Cell Environ. 29, 1508–1518. https://doi.org/10.1111/j.1365-3040.2006.01528.x

Li, F, Lei, H.J., Zhao, X.J., Tian, R.R., Li, T.H., 2012. Characterization of three sorbitol transporter genes in micropropagated apple plants grown under drought stress. Plant Mol. Biol. Report.30, 123-130. https://doi.org/10.1007/s11105-011-0323-4

Liu, H., Yu, L., Luo, Y., Wang, X., Huang, G., 2011. Responses of winter wheat (*Triticum aestivum L.*) evapotranspiration and yield to sprinkler irrigation regimes. Agric. Water Manag. 98, 483–492. https://doi.org/10.1016/j.agwat.2010.09.006

Lotfi, N.; Vahdati, K.; Hassani, D.; Kholdebarin, B.; Amiri, R., 2010. Peroxidase, guaiacol peroxidase and ascorbate peroxidase activity accumulation in leaves and roots of walnut trees in response to drought stress. Acta Hortic., 861, 309–316. doi:10.17660/ActaHortic.2010.861.42

Lopez, G., Pallas, B., Martinez, S., Lauri, P.É., Regnard, J.L., Durel, C.E., Costes, E., 2017. Heritability and genetic variation of plant biomass, transpiration, and water use efficiency for an apple core-collection. Acta Hortic. 1172, 317–322. https://doi.org/10.17660/ActaHortic.2017.1172.59

Lopez, G., Boini, A., Manfrini, L., Torres-Ruiz, J. M., Pierpaoli, E., Zibordi, M., Losciale, P., Morandi, B., Corelli-Grappadelli, L., 2018. Effect of shading and water stress on light interception, physiology and yield of apple trees. Agric. Water Manag. 210, 140-148. https://doi.org/10.1016/j.agwat.2018.08.015

Ludovisi, R., Tauro, F., Salvati, R., Khoury, S., Mugnozza Scarascia, G., Harfouche, A., 2017. UAV-based thermal imaging for high-throughput field phenotyping of black poplar response to drought. Frontiers Plant Sci., 8, 1681. doi:10.3389/fpls.2017.01681

Maes, W.H., Steppe, K., 2012. Estimating evapotranspiration and drought stress with ground-based thermal remote sensing in agriculture: a review. J. Exp. Bot. 63, 4671–4712. https://doi.org/10.1093/jxb/ers165

Maracchi, G., Sirotenko, O., & Bindi, M., 2005. Impacts of present and future climate variability on agriculture and forestry in the temperate regions: Europe. Clim. Change 70, 117–135. https://doi.org/10.1007/s10584-005-5939-7

Martinez-Gimeno, M.A., Castiella, M., Ruger, S., Intrigliolo, D.S., Ballester, C., 2017. Evaluating the usefulness of continuous leaf turgor pressure measurements for the assessment of Persimmon tree water status. Irrig. Sci. 35, 159-167. https://doi.org/10.1007/s00271-016-0527-3

Massonnet, C., Costes, E., Rambal, S., Dreyer, E., & Regnard, J.L., 2007. Stomatal regulation of photosynthesis in apple leaves: Evidence for different water-use strategies between two cultivars. Ann. Bot. 100, 1347–1356. https://doi.org/10.1093/aob/mcm222

McDowell, N.G., 2011. Mechanisms linking drought, hydraulics, carbon metabolism, and vegetation mortality. Plant Physiol. 155, 1051-1059. https://doi.org/10.1104/pp.110.170704

Naor, A., 2006. Irrigation scheduling and evaluation of tree water status in deciduous orchards. Hortic. Rev. 32, 111–165.

Ngao, J., Adam, B., Saudreau, M., 2017. Intra-crown spatial variability of leaf temperature and stomatal conductance enhanced by drought in apple tree as assessed by the RATP model. Agric. For. Meteorol. 237, 340-354. https://doi.org/10.1016/j.agrformet.2017.02.036

Pagay, V., 2021. Dynamic aspects of plant water potential revealed by a microtensiometer. BioRxiv, July 5, 2021. https://doi.org/10.1101/2021.06.23.449675

Parajuli, R., Thoma, G., Matlock, M.D., 2019. Environmental sustainability of fruit and vegetable production supply chains in the face of climate change: A review. Sci. Total Environ. 650, 2863–2879. https://doi.org/10.1016/j.scitotenv.2018.10.019

Pretorius, J.J.B., Wand, S.J.E., 2003. Late-season stomatal sensitivity to microclimate is influenced by sink strength and soil moisture stress in "Braestar" apple trees in South Africa. Sci. Hortic. 98, 157–171. https://doi.org/10.1016/s0304-4238(02)00209-1

Rahmati, M., Mirás-Avalos, J.M., Valsesia, P., Lescourret, F., Génard, M., Davarynejad, G.H., Bannayan, M., Azizi, M., Vercambre, G., 2018. Disentangling the effects of water stress on carbon acquisition, vegetative growth, and fruit quality of peach trees by means of the QualiTree model. Front. Plant Sci. 9, 3. https://doi.org/10.3389/fpls.2018.00003

Regnard, J.L., Ducrey, M., Porteix, E., Segura, V., Costes, E., 2008. Phenotyping apple progeny for ecophysiological traits: how and what for? Acta Hort. 772, 151–158. https://doi.org/10.17660/actahortic.2008.772.18

Rischbeck, P., Cardellach, P., Mistele, B., Schmidhalter, U., 2017. Thermal phenotyping of stomatal sensitivity in spring barley. J. Agron. Crop Sci. 203, 483–493. https://doi.org/10.1111/jac.12223

Robinson, C., Clay, D.E., Clay, S.A., Bruggeman, S.A., 2017. Calculating the impacts of agriculture on the environment and how precision farming can reduce these consequences. In: Clay, D.E., Clay S.A., Bruggeman S.A. (Eds), Practical

617 mathematics for precision farming, chapter 18, pp. 247-261, ACSESS Publications, Wiley.
618 https://doi.org/10.2134/practicalmath2017.0108
619 Sánchez-Virosta, Á., Sánchez-Gómez, D., 2020. Thermography as a tool to assess inter-cultivar variability in garlic
620 performance along variations of soil water availability. Remote Sens. 12, 2990. https://doi.org/10.3390/rs12182990
621 Schultz, H.R., 2003. Differences in hydraulic architecture account for near-isohydric and anisohydric behaviour of two field-
622 grown *Vitis vinifera* L. cultivars during drought. Plant Cell Environ. 26, 1393-1405. https://doi.org/10.1046/j.1365-
623 3040.2003.01064.x
624 Simonin, K.A., Burns, E., Choat, B., Barbour, M.M., Dawson, T.E., Franks, P.J., 2014. Increasing leaf hydraulic conductance
625 with transpiration rate minimizes the water potential drawdown from stem to leaf. J. Exp. Bot. 66, 1303-1315.
626 https://doi.org/10.1093/jxb/eru481
627 Šircelj, H., Tausz, M., Grill, D., Batič, F., 2007. Detecting different levels of drought stress in apple trees (Malus domestica
628 *Borkh*) with selected biochemical and physiological parameters. Sci. Hortic. 113, 362–369.
629 https://doi.org/10.1016/j.scienta.2007.04.012
630 Steduto P., Hsiao T.C., Fereres E., Raes D., 2012. Crop yield response to water. Irrigation and drainage Paper 66, FAO, Rome.
631 Tardieu, F., Simonneau, T., 1998. Variability among species of stomatal control under fluctuating soil water status and
632 evaporative demand: modelling isohydric and anisohydric behaviours. J. Exp. Bot. 49, 419-432.
633 https://doi.org/10.1093/jexbot/49.suppl_1.419
634 Thompson, A.L., Thorp, K.R., Conley, M., Andrade-Sanchez, P., Heun, J.T., Dyer, J.M., White, J.W., 2018. Deploying a
635 proximal sensing cart to identify drought-adaptive traits in upland cotton for high-throughput phenotyping. Front. Plant
636 Sci. 9, 507. https://doi.org/10.3389/fpls.2018.00507
637 Tripathi A., Tripathi D.K., Chauhan D.K., Kumar N., Singh G.S., 2016. Paradigms of climate change impacts on some major
638 food sources of the world: A review on current knowledge and future prospects. Agric. Ecosyst. Environ. 216, 356-373.
639 https://doi.org/10.1016/j.agee.2015.09.034
640 Virlet, N., Costes, E., Martinez, S., Kelner, J.J., Regnard, J.L., 2015. Multispectral airborne imagery in the field reveals genetic
641 determinisms of morphological and transpiration traits of an apple tree hybrid population in response to water deficit. J. of
642 Exp. Bot. 66(18), 5453-5465. https://doi.org/10.1093/jxb/erv355
643 Wang, D., Gartung, J., 2010. Infrared canopy temperature of early-ripening peach trees under postharvest deficit irrigation.
644 Agric. Water Manag. 97, 1787-1794. https://doi.org/10.1016/j.agwat.2010.06.014
645 White, J.W., Andrade-Sanchez, P., Gore, M.A., Bronson, K.F., Coffelt, T.A., Conley, M.M., Feldmann, K.A., French, A.N.,
646 Heun, J.T., Hunsaker, D.J., et al., 2012. Field-based phenomics for plant genetics research. Field Crops Res. 133, 101–112.
647 https://doi.org/10.1016/j.fcr.2012.04.003
648

649 **FIGURES**

650

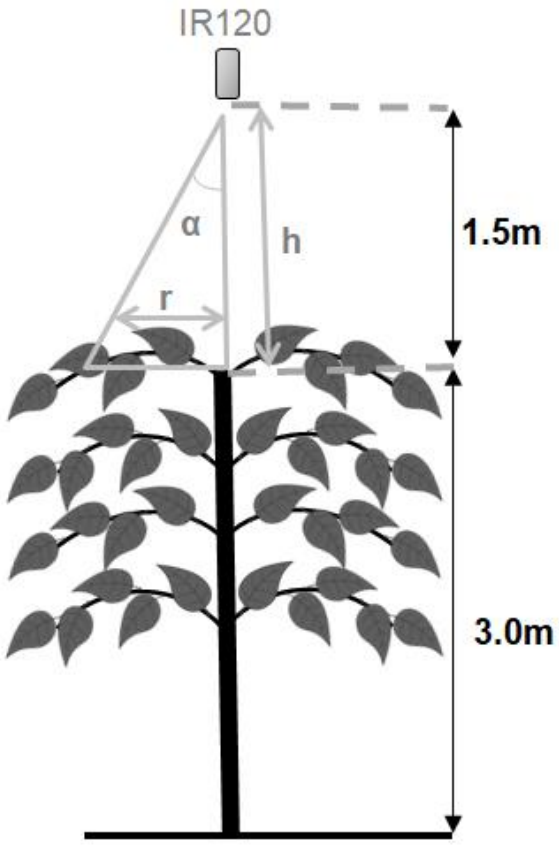

651

652 **Fig. 1.** Schematic representation of the IR120 thermo-radiometer position placed above the apple tree
653 canopy. The IR120 sensor is measuring the canopy temperature (Ts ≈ Tbr) continuously from a zenithal
654 view (half angle α= 20°, see text).

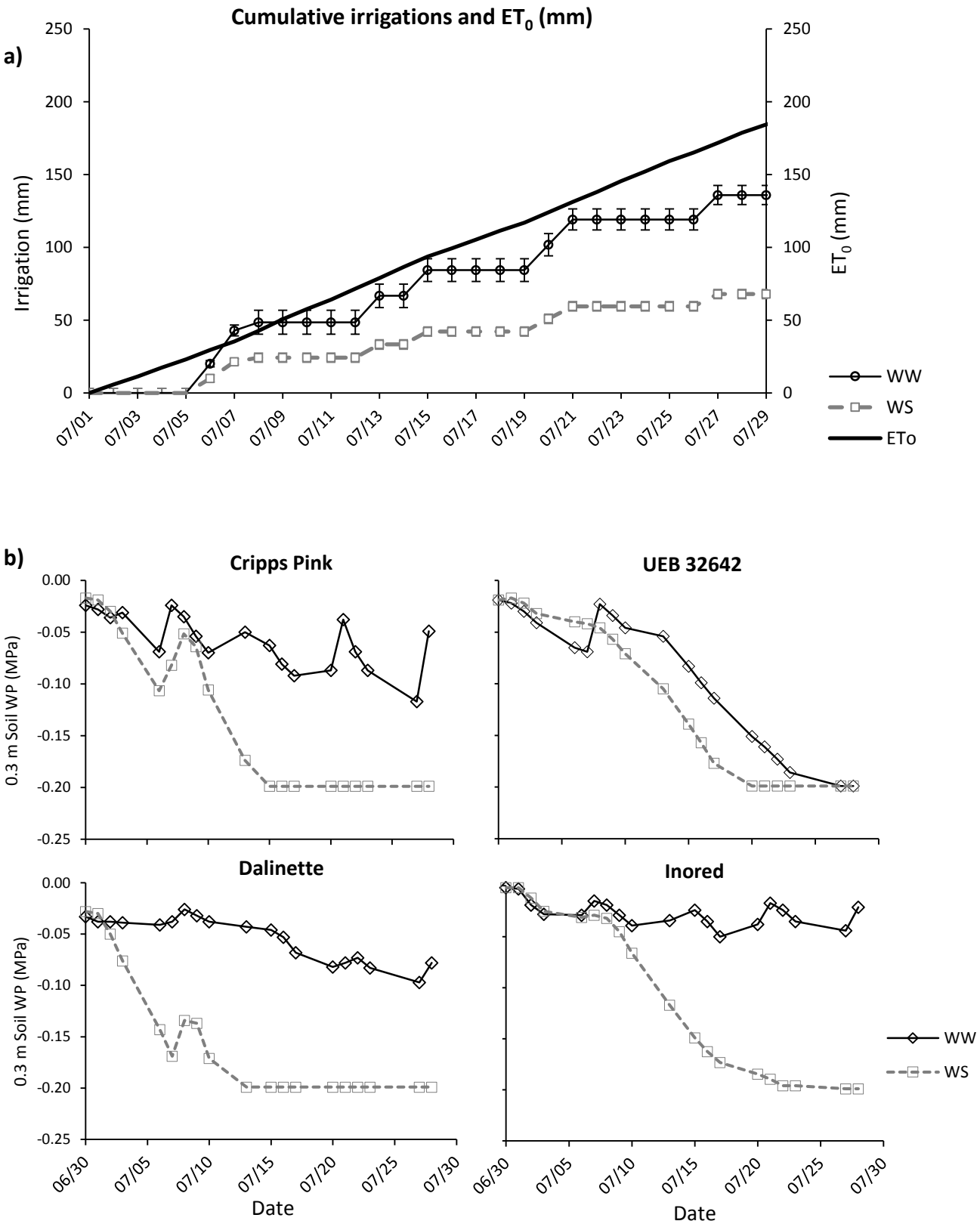

Fig. 2. Seasonal changes resulting from the two irrigation treatments, control irrigation (WW) and increasing water deficit (WS). **a)** Cumulative evapotranspiration (ET_0) and irrigation (mean and standard deviation, for 6 apple varieties). **b)** Soil water potential (Soil WP) measured at -0.3 m (median values of 3 probes, for 4 apple varieties). The solid black lines represent the evolution of Soil WP on WW trees, and the dashed grey lines the evolution on WS trees.

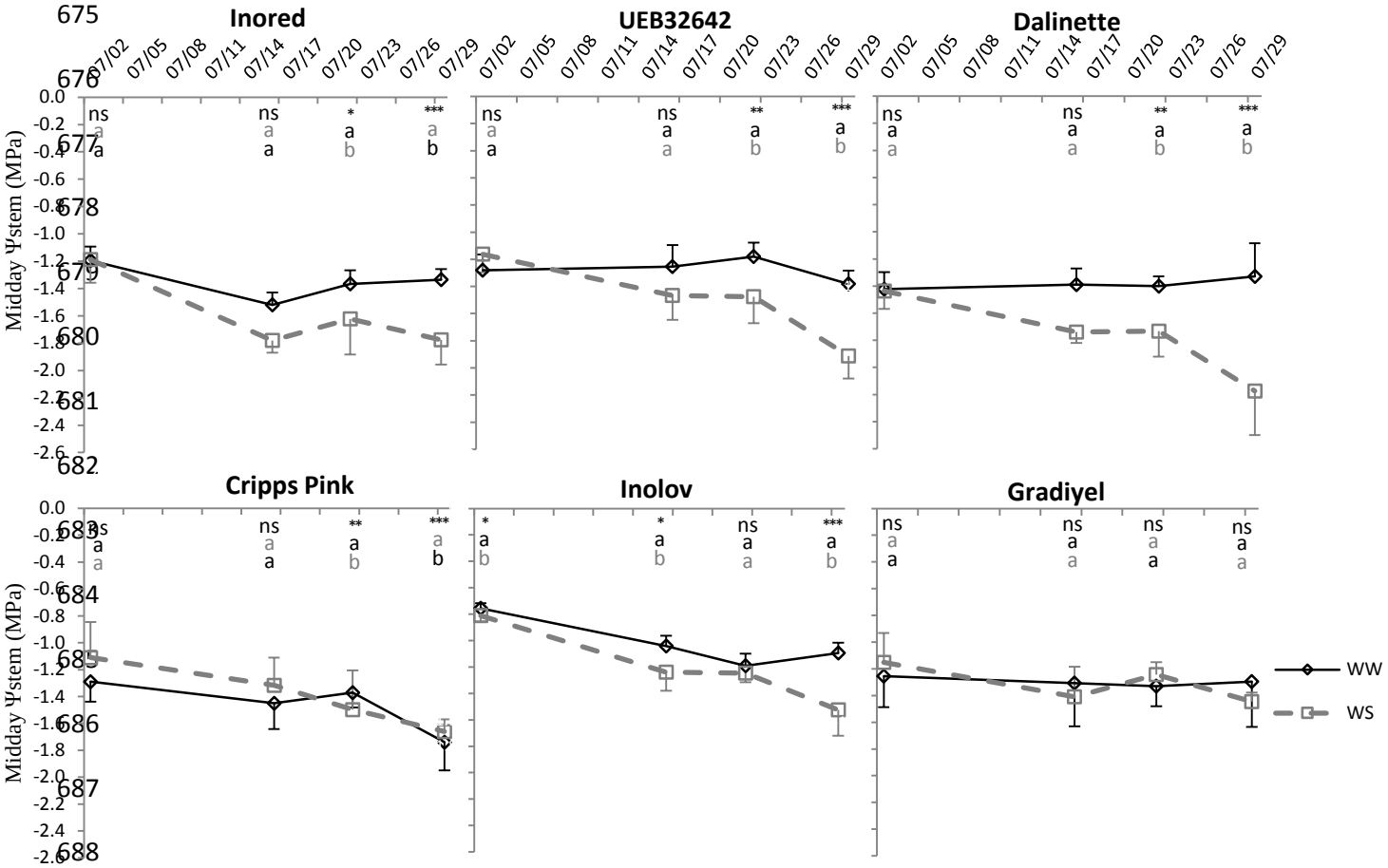

Fig. 3. Stem water potential (Ψstem, MPa) measured at solar midday (12:00 GMT) in July 2015 on 6 apple tree varieties (mean values and standard deviations, 3 leaves x 2 trees per variety). The solid black lines represent the Ψstem evolution on control trees (WW) not water rationed, and the dashed grey lines its evolution on trees under increasing water deficit (WS) trees. The significant effect of watering treatment is described by symbols: "ns" ($P > 0.05$), "*" ($P < 0.05$), "**" ($P < 0.01$), "***" ($P < 0.001$), and differences are indicated by different letters.

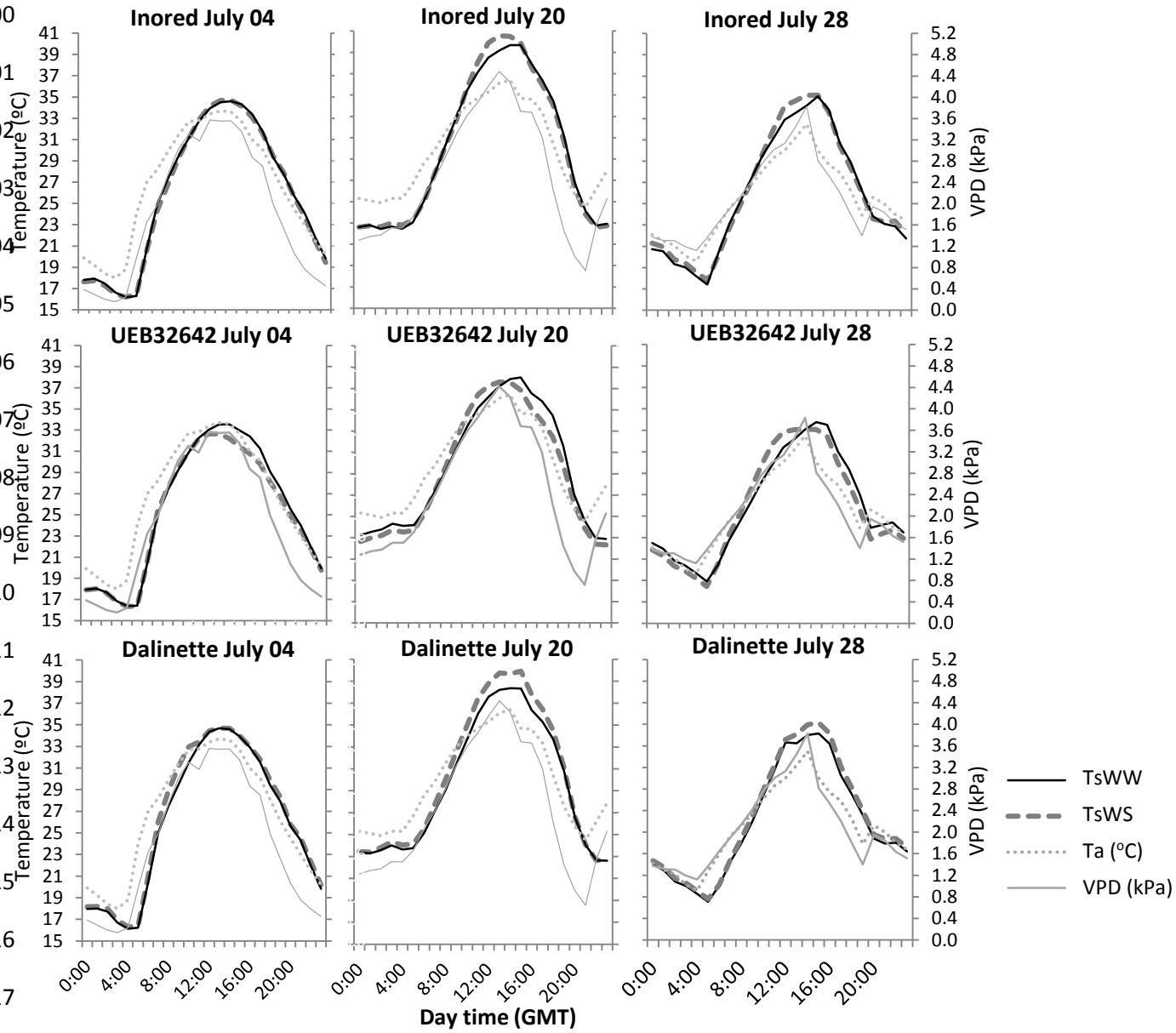

Fig. 4.a. Thermal response of apple canopy (Inored, UEB32642 and Dalinette varieties) to contrasting irrigation regimes. The thin solid black lines represent the canopy surface temperature (Ts) evolution for control irrigation (WW) trees, and the thick dashed grey lines represent the Ts evolution for increasing water deficits (WS) trees. The three dates shown correspond to progressive soil water deficits on WS trees in cloudless days. The thin solid grey line is relative to air Vapor Pressure Deficit (VPD) and the thin dashed grey line is relative to the air temperature (Ta).

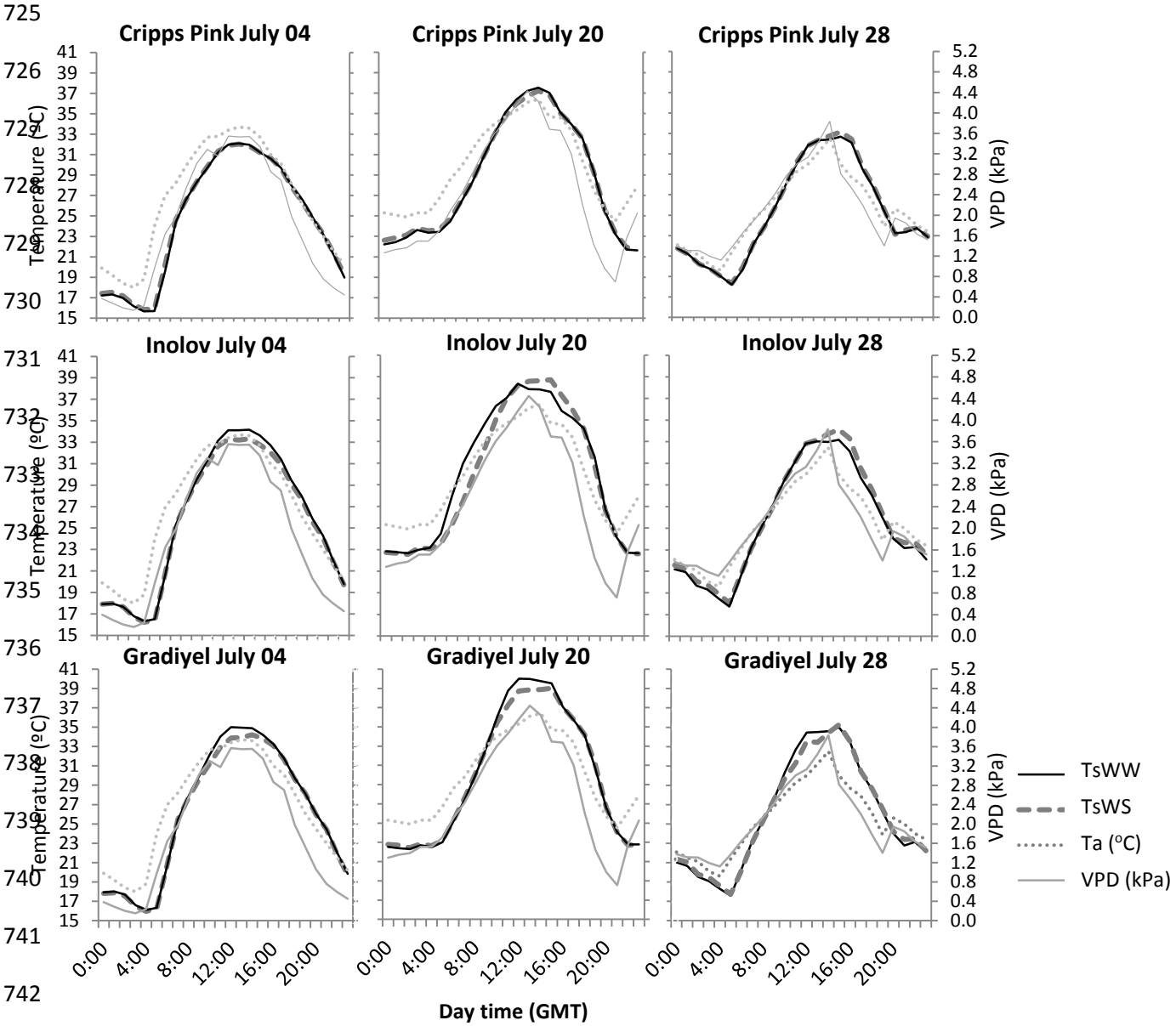

Fig. 4.b. Thermal response of apple canopy (Cripps Pink, Inolov and Gradiyel varieties) to contrasting irrigation regimes. The thin solid black lines represent the canopy surface temperature (Ts) evolution for control irrigation (WW) trees, and the thick dashed grey lines the Ts evolution for increasing water deficits (WS) trees. The three dates shown correspond to progressive soil water deficits on WS trees in cloudless days. The thin solid grey line is relative to air Vapor Pressure Deficit (VPD) and the thin dashed grey line to the air temperature (Ta).

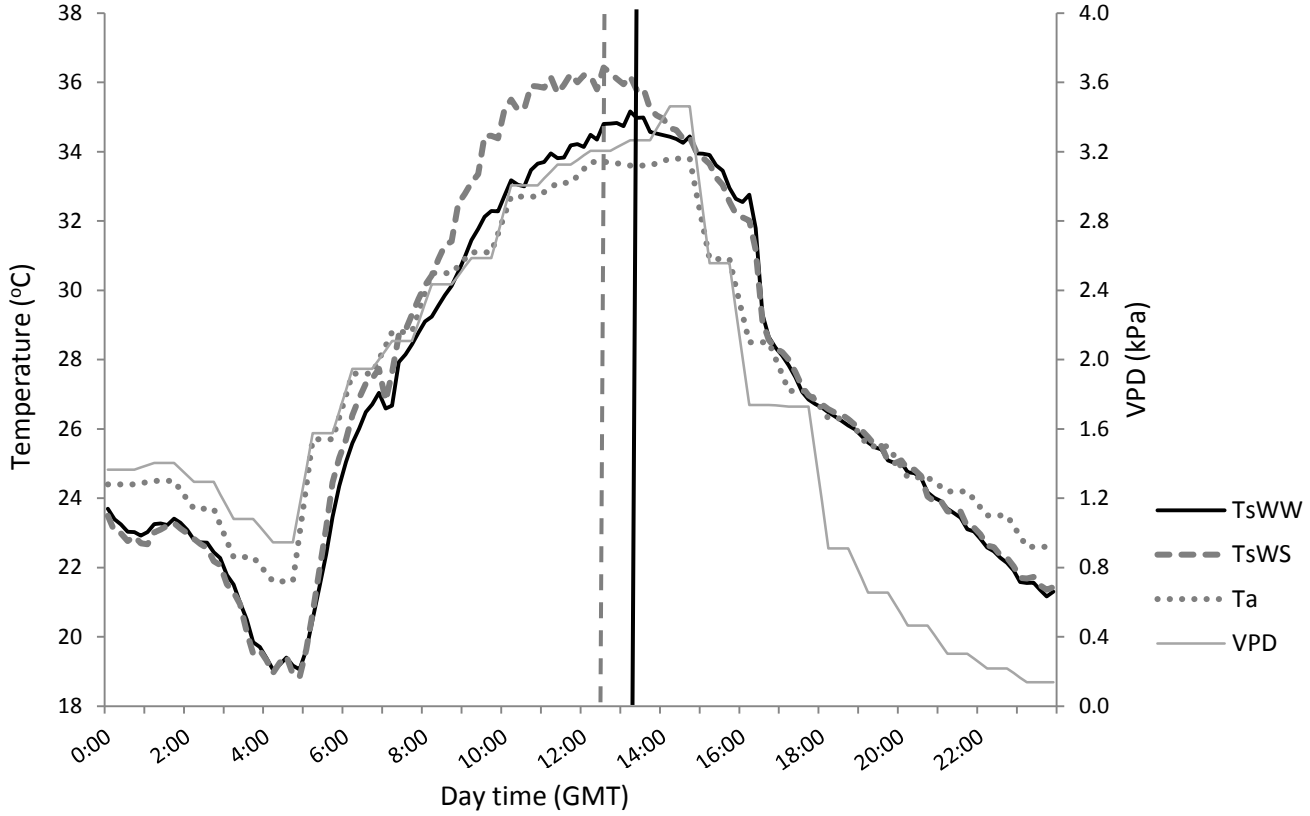

749

750 **Fig. 5.** Daily evolution of tree canopy surface temperature (Ts) for UEB32642 apple variety in response
751 to WW and WS irrigation regimes (example shown, July 24). The thick black line represents the Ts
752 evolution on control irrigation (WW) trees, and the thick dashed grey line shows the Ts evolution on
753 soil water deficit (WS) trees. TsWW and TsWS are average values at a 10 min time step. The dotted
754 grey line is relative to the air temperature (Ta) and the thin solid grey line is relative to the air Vapor
755 Pressure Deficit (VPD), both obtained by the local weather station at a 1h time step. VPD is computed
756 according to Buck (1981). The time corresponding to the maximum Ts observed for the WW and WS
757 trees is indicated by a vertical line (solid black line and dashed grey line, respectively).

758

759

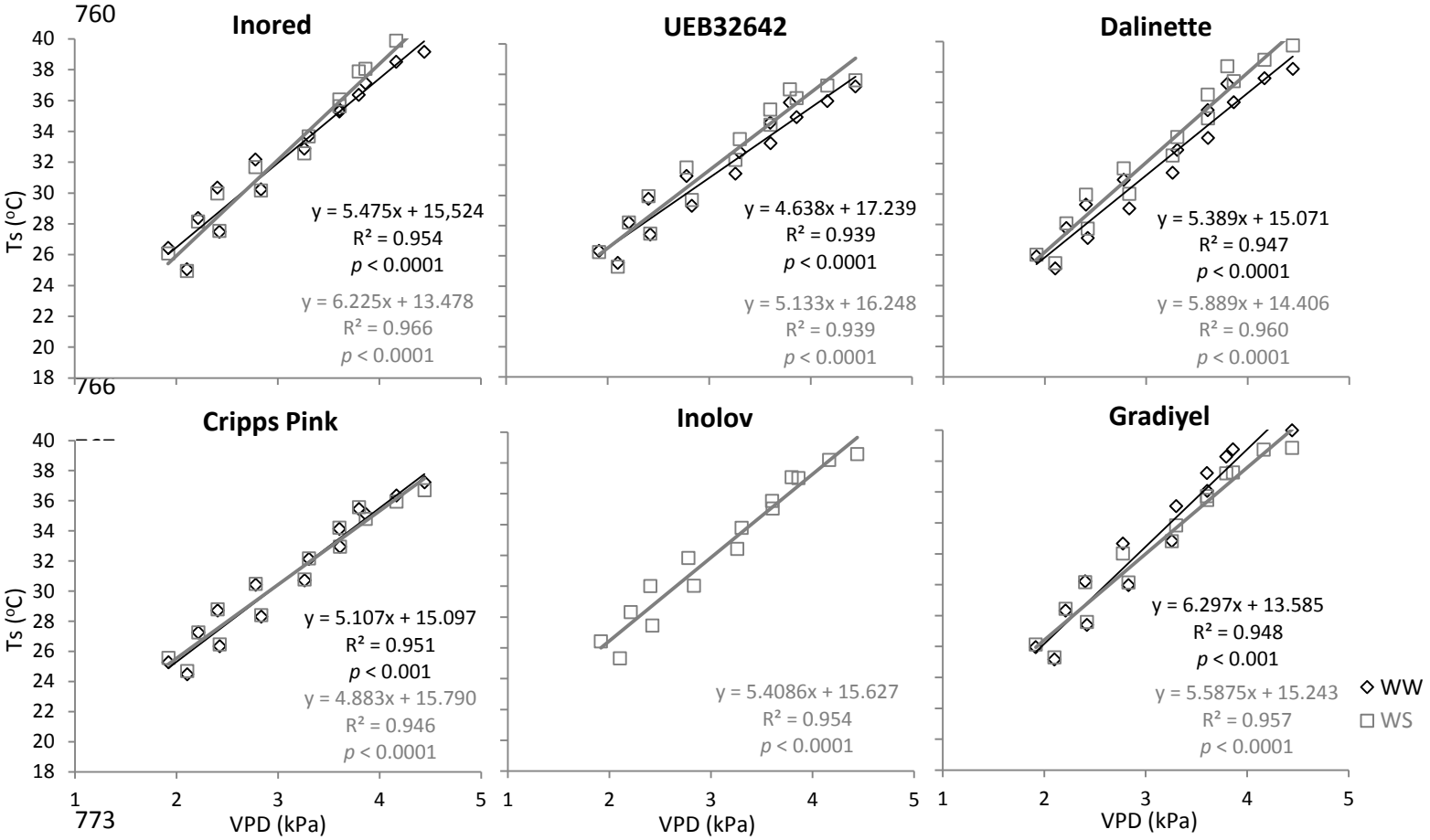

Fig. 6.a. Linear relationships between air Vapor Pressure Deficit (VPD) and canopy surface temperature (Ts) for 6 apple varieties during the diurnal period from 06:00 to 13:00 (data for July 20-21). Black markers and solid lines are relative to control irrigation (WW) trees, and grey markers and thick solid lines are relative to soil water deficit (WS) trees. The regression line equations for the WW tree response to VPD are written in black, while those for the WS trees are in grey. Ts outliers observed WW on the Inolov variety at these dates are not presented here (only in Table S1).

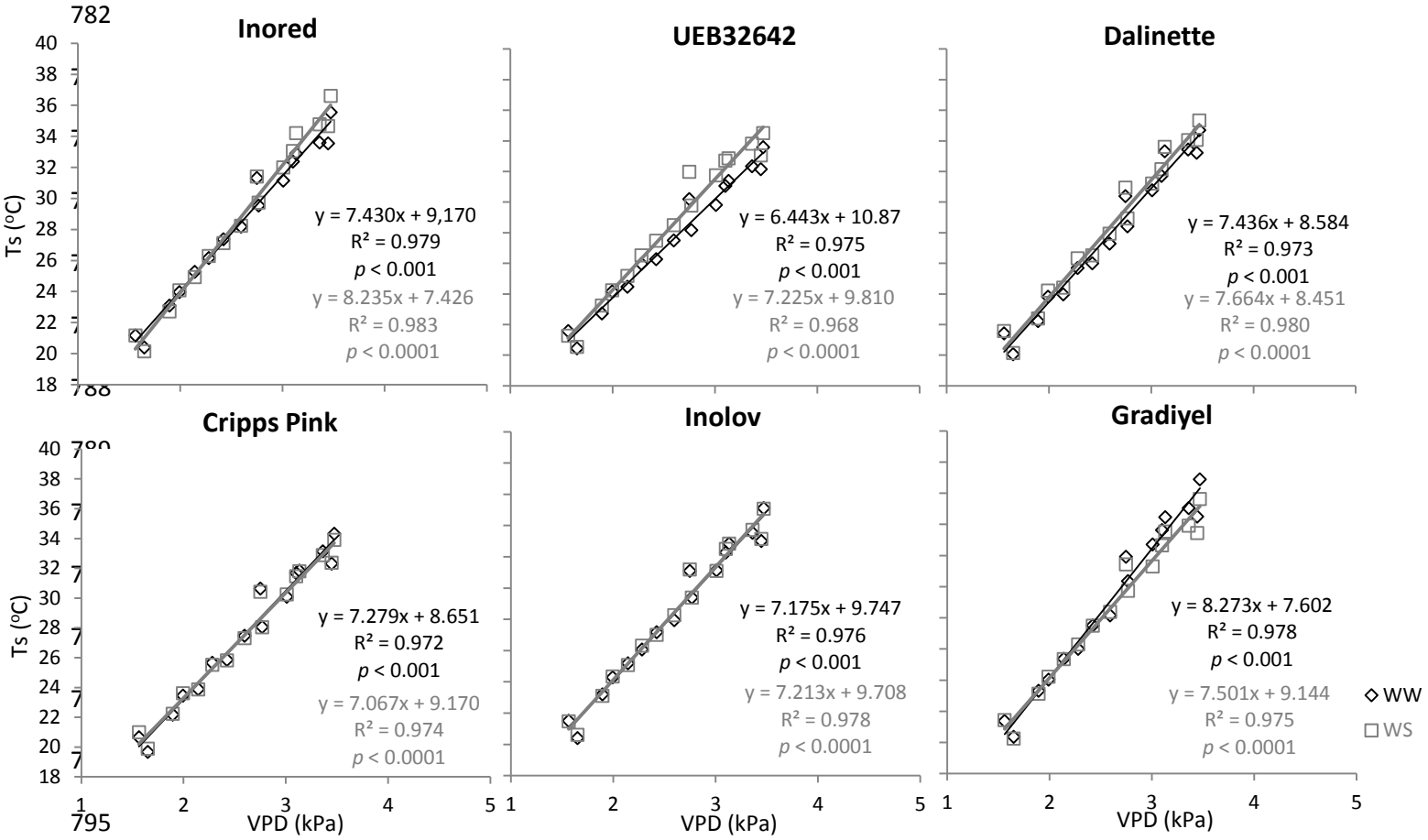

Fig. 6.b. Linear relationships between air Vapor Pressure Deficit (VPD) and canopy surface temperature (Ts) for 6 apple varieties during the diurnal period from 06:00 to 13:00 (data for July 27-28). Black markers and solid lines are relative to control irrigation (WW) trees, and grey markers and thick solid lines are relative to soil water deficit (WS) trees. The regression line equations for the WW tree response to VPD are written in black, while those for the WS trees are in grey.

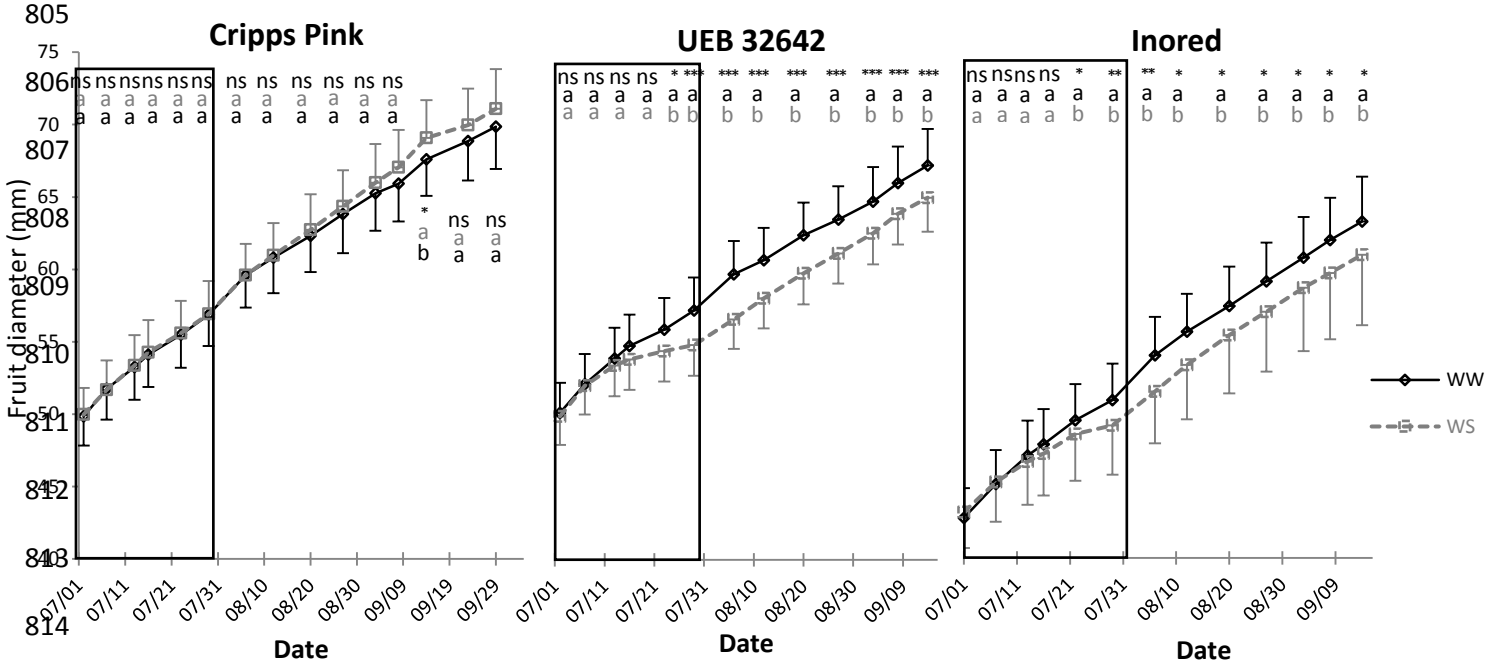

Fig. 7. Cumulative fruit growth for three apple varieties. Solid black lines are relative to the equatorial fruit diameter (mean and standard deviation, n=30) of control irrigation (WW) trees, and thick dashed grey lines are relative to equatorial fruit diameter of trees subjected to increasing soil water deficits (WS) in July. Rectangular areas correspond to the water restriction period. The significant effect of irrigation regime is described by symbols: "ns" ($P > 0.05$), "*" ($P < 0.05$), "**" ($P < 0.01$), "***" ($P < 0.001$), and differences are indicated by different letters.

TABLES

Table 1. Mean canopy surface temperature (Ts) around solar midday (11:50-12:00 GMT) measured by IR120 sensors on control irrigation (WW) and increasing water deficit (WS) trees for 6 apple varieties. The three dates presented refer to full sunny days, 14, 20 and 27 days after the establishment of contrasting irrigation regimes, days for which the air temperature at midday was 29.9, 33.6 and 30.8 ºC respectively.

Variety	Treatment	Mean canopy surface temperature (Ts ± s.d., ºC)		
		July 16	July 22	July 29
Cripps Pink	WW	32.2±0.21	34.2±0.32	31.9±0.74
	WS	32.1±0.19	34.5±0.19	32.2±0.97
UEB32642	WW	32.1±0.23	34.5±0.32	32.5±0.58
	WS	32.9±0.15	35.8±0.38	33.9±1.04
Dalinette	WW	33.2±0.30	35.4±0.51	33.6±0.83
	WS	35.2±0.36	36.7±0.52	35.0±1.04
Inored	WW	32.2±0.17	35.3±0.19	32.7±0.42
	WS	34.2±0.24	37.0±0.19	34.4±0.68
Inolov	WW	32.5±0.28	34.8±0.32	32.3±0.66
	WS	33.3±0.33	36.0±0.04	33.6±0.79
Gradiyel	WW	32.6±0.27	35.0±0.17	32.9±0.76
	WS	33.5±0.28	35.7±0.13	33.0±0.65
Effect of water regime		ns	ns	ns

The significance of irrigation regime effect by One Way ANOVA test (α=0.05) is described by symbols: "ns" ($P > 0.05$), "*" ($P < 0.05$), "**" ($P < 0.01$), "***" ($P < 0.001$)

Table 2. Time of maximum canopy surface temperature (GMT time) for 6 apple tree varieties under control irrigation (WW) and increasing water deficit (WS) irrigation regimes. The thermal difference (ΔT_{max}) between the maximum reached (TsWS-TsWW) regardless of time is also indicated. The three dates presented refer to full sunny days, 14, 20 and 27 days after the establishment of the contrasting irrigation regimes.

Variety	Irrigation regime	July 16		July 22		July 29	
		$Time_{max}$ (h)	ΔT_{max} (ºC)	$Time_{max}$ (h)	ΔT_{max} (ºC)	$Time_{max}$ (h)	ΔT_{max} (ºC)
Cripps Pink	WW	12:00		11:20		13:40	
	WS	12:00	0.00	11:00	0.20	13:40	0.88
UEB32642	WW	13:20		11:10		13:40	
	WS	11:10	0.83	11:10	1.25	11:40	1.28
Dalinette	WW	12:10		11:10		13:40	
	WS	12:10	1.33	11:00	1.00	13:40	1.49
Inored	WW	13:30		14:20		13:30	
	WS	12:40	1.19	11:00	1.33	11:40	1.05
Inolov	WW	11:00		11:00		13:30	
	WS	11:00	1.31	11:00	0.53	13:30	1.42
Gradiyel	WW	12:10		11:00		13:40	
	WS	12:30	-0.72	11:00	-0.73	13:40	0.04

838 **Table 3.** Average tree fruit load and yield components at harvest for 6 apple varieties submitted in July
839 to two contrasting control irrigation (WW) and water deficit (WS) irrigation regimes (means ± s.d., for
840 3 trees).

Variety (Harvest date)	Irrigation regime	Fruit load	Individual fruit weight (g)	Yield per tree (kg)
Cripps Pink	WW	198±28[a]	153.5±8.6[b]	30.3±3.6[a]
(Oct. 10th)	WS	182±33[a]	168.5±3.4[a]	30.6±5.8[a]
UEB32642	WW	285±52[a]	141.3±7.7[a]	40.2±7.0[a]
(Sept. 15th)	WS	283±79[a]	134.2±6.8[a]	37.5±8.0[a]
Dalinette	WW	235±44[a]	177.1±2.9[a]	40.9±3.2[a]
(Oct. 21st)	WS	233±47[a]	165.9±22.8[a]	38.0±4.1[a]
Inored	WW	261±70[a]	122.3±5.8[a]	31.9±1.1[a]
(Sept. 22nd)	WS	262±73[a]	107.3±3.4[b]	28.0±7.2[a]
Inolov	WW	174±16[a]	129.5±2.6[a]	22.6±3.5[a]
(Sept. 15th)	WS	151±31[a]	127.7±5.7[a]	19.2±3.1[a]
Gradiyel	WW	269±63[a]	149.4±3.0[a]	40.1±8.9[a]
(Oct. 13rd)	WS	253±110[a]	150.6±5.3[a]	38.4±18.0[a]

841 Significant differences at harvest between treatments for each variety are indicated by different letters
842 according to the One Way ANOVA test (α=0.05).

843
844
845

SUPPLEMENTARY MATERIAL

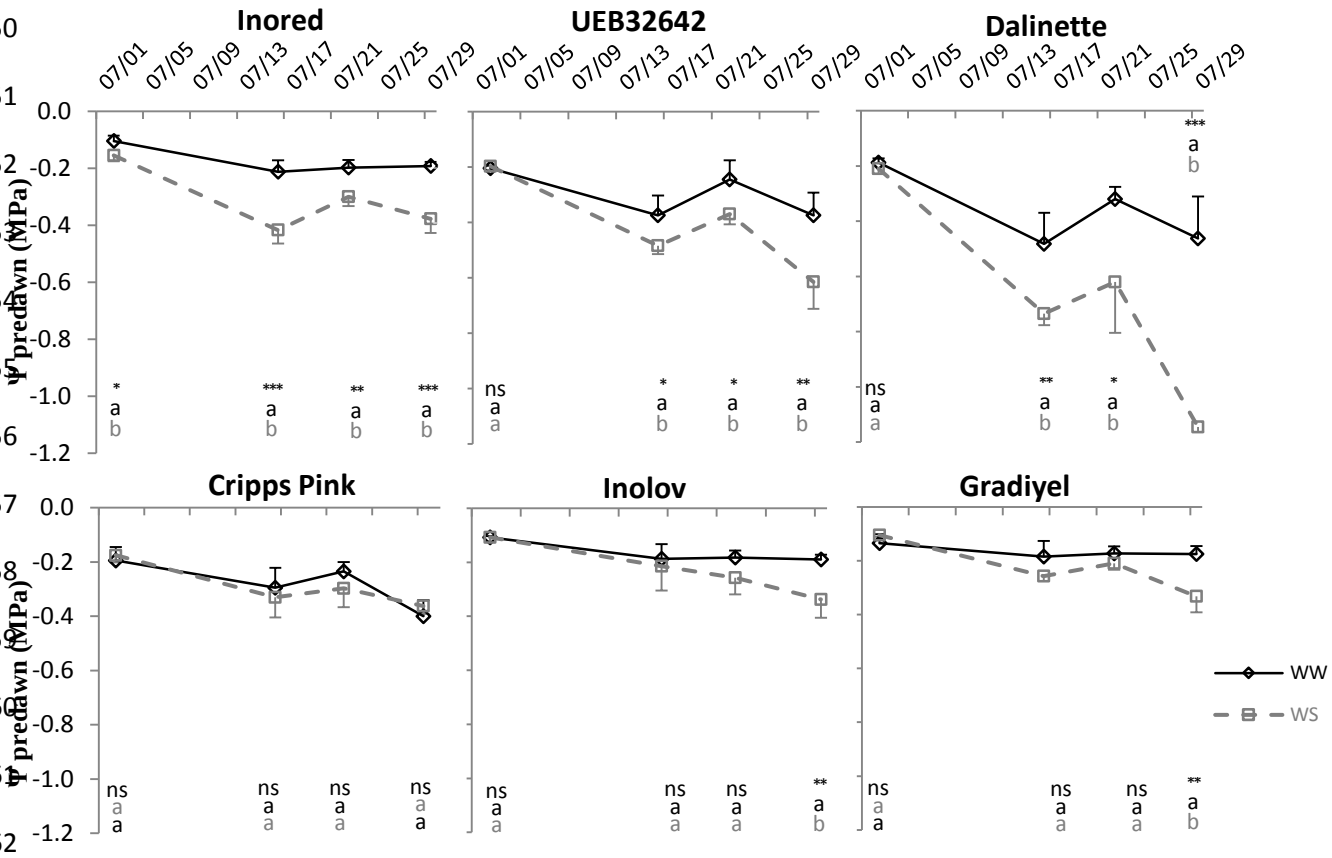

Fig. S1. Seasonal evolution of tree predawn water potential (Ψpredawn) for 6 apple varieties; measurements in July 2015 at 3:00 GMT (means and standard deviations, 2 trees x 2 leaves). Black solid lines represent the evolution of Ψpredawn on control irrigation (WW) trees, and thick grey dashed lines represent the evolution of Ψpredawn on increasing water deficits (WS) trees. The significant effect of irrigation regime is described by symbols: "ns" ($P > 0.05$), "*" ($P < 0.05$), "**" ($P < 0.01$), "***" ($P < 0.001$), and differences indicated by different letters.

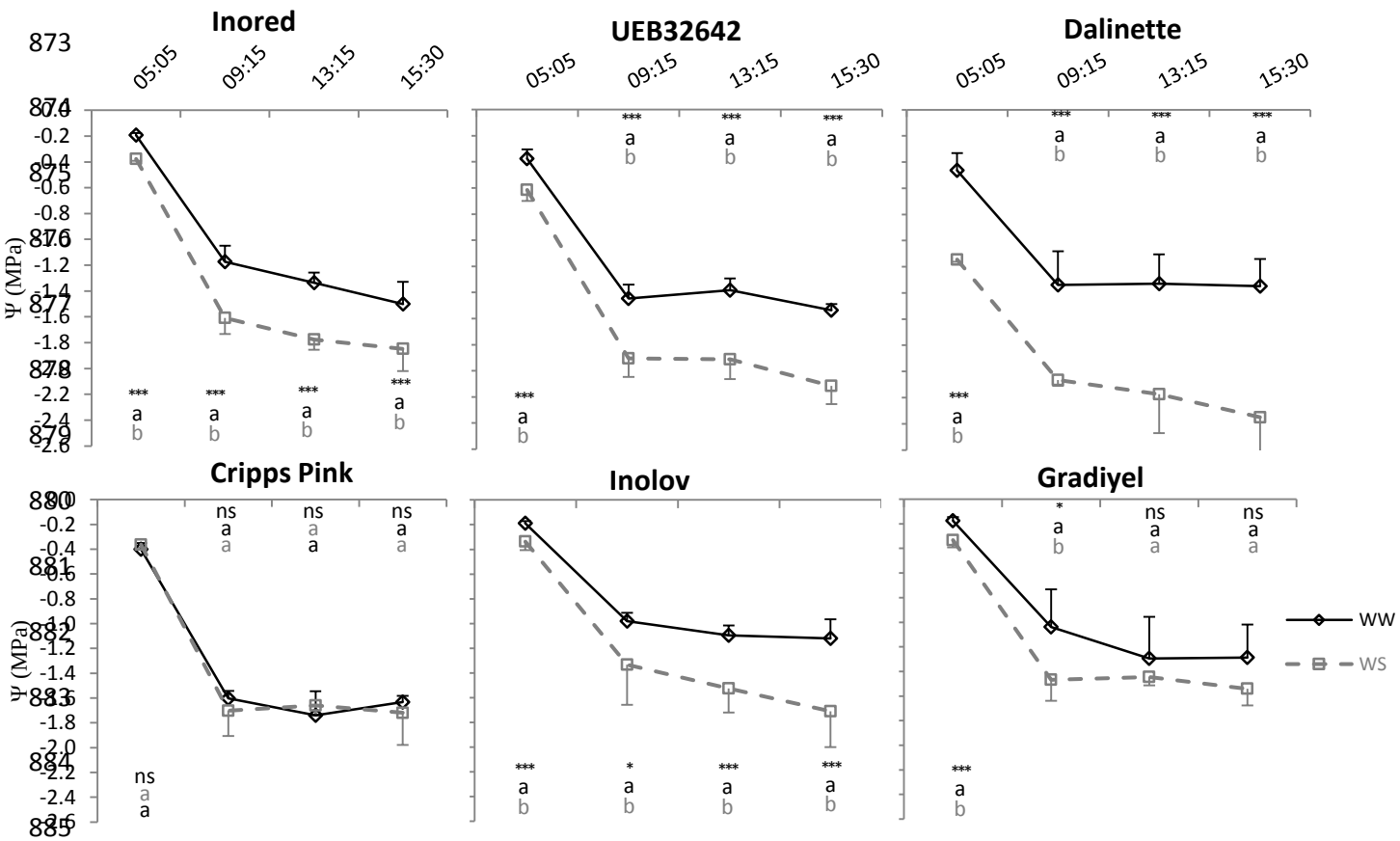

Fig. S2. Daily evolution of water potential (Ψ) on apple trees (July 29) for 6 varieties (means and standard deviations, 2 trees x 3 leaves). The first hour of measurement corresponds to Ψ predawn whereas subsequent measurements correspond to diurnal Ψ stem. The solid black lines are relative to Ψ evolution on control irrigation (WW) trees, and the thick grey dashed lines to Ψ evolution on water deficit (WS) trees. The significant effect of irrigation regime is described by symbols: "ns" ($P > 0.05$), "*" ($P < 0.05$), "**" ($P < 0.01$), "***" ($P < 0.001$), and differences are indicated by different letters.

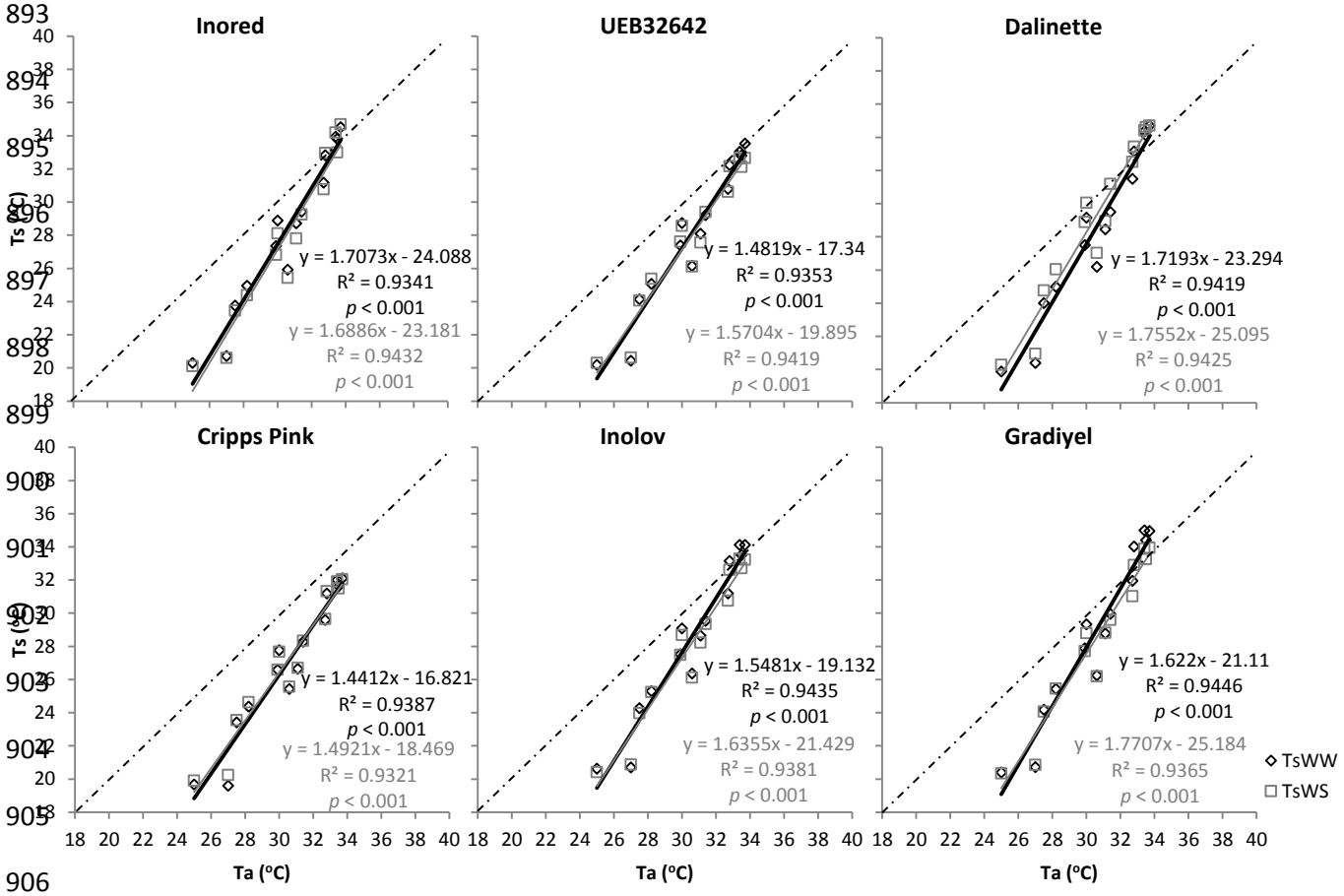

Fig. S3.a Linear relationships between air temperature (Ta) and canopy surface temperature (Ts) for 6 apple varieties during the diurnal period from 06:00 to 13:00 (data for July 3-4). Black markers and solid lines are relative to control irrigation (WW) trees, and grey markers and thick solid lines are relative to soil water deficit (WS) trees. Theoretical Ts:Ta 1:1 lines are drawn as dash-dotted. The regression line equations for the WW tree response to Vapor Pressure Deficit are written in black, while those for the WS trees are in grey.

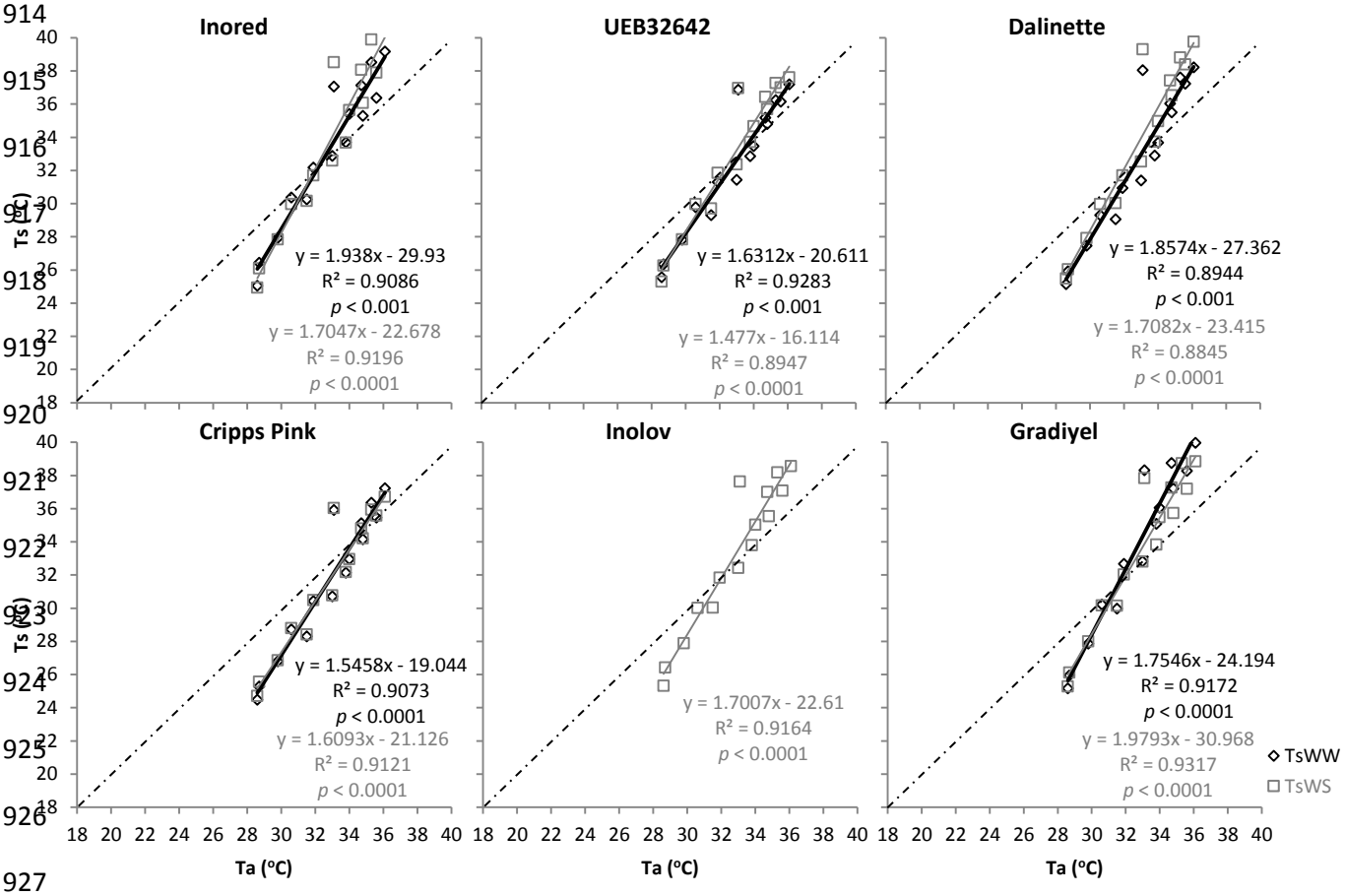

Fig. S3.b Linear relationships between air temperature (Ta) and canopy surface temperature (Ts) for 6 apple varieties during the diurnal period from 06:00 to 13:00 (data for July 20-21). Black markers and solid lines are relative to control irrigation (WW) trees, and grey markers and thick solid lines are relative to soil water deficit (WS) trees. Theoretical Ts:Ta 1:1 lines are drawn as dash-dotted. The regression line equations for the WW tree response to Vapor Pressure Deficit are written in black, while those for the WS trees are in grey.

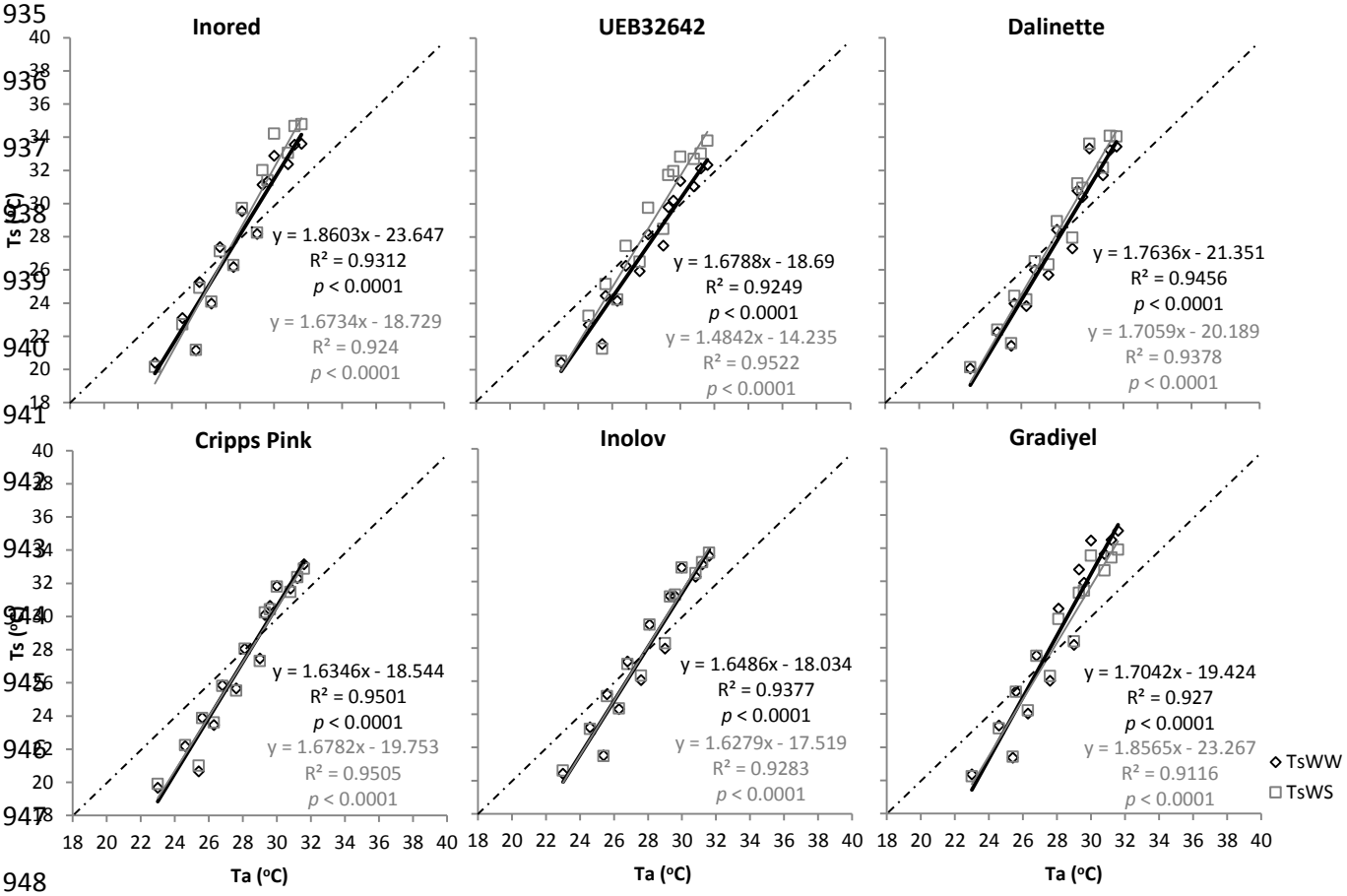

Fig. S3.c Linear relationships between air temperature (Ta) and canopy surface temperature (Ts) for 6 apple varieties during the diurnal period from 06:00 to 13:00 (data for July 27-28). Black markers and solid lines are relative to control irrigation (WW) trees, and grey markers and thick solid lines are relative to soil water deficit (WS) trees. Theoretical Ts:Ta 1:1 lines are drawn as dash-dotted. The regression line equations for the WW tree response to Vapor Pressure Deficit are written in black, while those for the WS trees are in grey.

957

958 **Table S1:** Linear equations and corresponding R^2 coefficients of Canopy Temperature as a function of
959 Vapor Pressure Deficit values during morning (06:00 to 13:00 GMT) and afternoon (13:00 to 19:00
960 GMT) periods on control irrigation (WW) and water deficit (WS) irrigation regimes. Dates correspond
961 to representative sunny days of (1) no stress (July 3, 4), (2) medium-term WS water restrictions (July
962 20, 21) and (3) final dates of WS water restrictions (July 27, 28).

Genotype	Date	Treatment	Morning		Afternoon	
			Linear Equation	R^2	Linear Equation	R^2
Inored	1	WW	5.901x + 12.832	0.945	3.439x + 22.660	0.961
		WS	5.939x + 12.359	0.944	3.363x + 22.231	0.924
	2	WW	5.475x + 15.524	0.954	2.879x + 27.819	0.870
		WS	6.225x + 13.478	0.966	3.258x + 27.053	0.834
	3	WW	7.430x + 9.170	0.979	4.064x + 21.254	0.760
		WS	8.235x + 7.426	0.983	4.537x + 19.928	0.834
UEB 32642	1	WW	5.450x + 13.687	0.939	2.936x + 23.151	0.965
		WS	5.133x + 14.371	0.936	2.844x + 22.059	0.974
	2	WW	4.638x + 17.239	0.939	2.103x + 29.487	0.753
		WS	5.133x + 16.248	0.939	2.472x + 27.457	0.747
	3	WW	6.443x + 10.871	0.975	2.699x + 24.236	0.678
		WS	7.225x + 9.814	0.968	3.508x + 21.272	0.786
Dalinette	1	WW	6.124x + 12.369	0.943	3.447x + 22.399	0.980
		WS	6.030x + 13.338	0.948	3.253x + 23.195	0.987
	2	WW	5.389x + 15.071	0.947	2.516x + 28.315	0.752
		WS	5.889x + 14.406	0.960	2.789x + 28.744	0.743
	3	WW	7.436x + 8.584	0.973	3.529x + 22.011	0.801
		WS	7.6641x + 8.450	0.977	3.627x + 22.421	0.784
Cripps Pink	1	WW	5.186x + 13.416	0.934	2.819x + 21.963	0.973
		WS	5.009x + 13.975	0.941	2.917x + 21.658	0.966
	2	WW	5.107x + 15.097	0.951	2.630x + 26.624	0.829
		WS	4.883x + 15.790	0.945	2.458x + 27.141	0.769
	3	WW	7.279x + 8.651	0.972	3.517x + 21.101	0.794
		WS	7.067x + 8.651	0.974	3.403x + 21.404	0.762
Inolov	1	WW	5.679x + 13.532	0.938	3.107x + 23.112	0.974
		WS	5.366x + 13.981	0.943	2.827x + 23.279	0.970
	2	WW	3.925x + 21.774	0.930	2.283x + 28.615	0.778
		WS	5.409x + 15.627	0.954	2.737x + 27.856	0.817
	3	WW	7.175x + 9.747	0.976	3.739x + 21.084	0.813
		WS	7.213x + 9.708	0.978	3.607x + 21.963	0.782
Gradiyel	1	WW	6.181x + 12.595	0.941	3.402x + 22.841	0.980
		WS	5.626x + 13.570	0.945	2.955x + 23.702	0.957
	2	WW	6.297x + 13.585	0.948	3.014x + 27.489	0.818
		WS	5.587x + 15.243	0.957	2.660x + 28.297	0.797
	3	WW	8.273x + 7.602	0.978	4.548x + 20.150	0.801
		WS	7.501x + 9.144	0.975	3.990x + 21.516	0.775

963